the plant journal

SEB SOCIETY FOR EXPERIMENTAL BIOLOGY

The Plant Journal (2019) doi: 10.1111/tpj.14503

The overexpression of rice ACYL-CoA-BINDING PROTEIN2 increases grain size and bran oil content in transgenic rice

Ze-Hua Guo[1], Richard P. Haslam[2], Louise V Michaelson[2], Edward C. Yeung[3], Shiu-Cheung Lung[1], Johnathan A. Napier[2] and Mee-Len Chye[1,4,*]

[1]*School of Biological Sciences, University of Hong Kong, Pokfulam, Hong Kong, China,*

[2]*Department of Plant Science, Rothamsted Research, Harpenden, Hertfordshire AL5 2JQ, UK,*

[3]*Department of Biological Sciences, University of Calgary, Calgary, AB, T2N 1N4, Canada, and*

[4]*State Key Laboratory of Agrobiotechnology, The Chinese University of Hong Kong, Shatin, NT, Hong Kong, China*

Received 13 May 2018; revised 27 July 2019; accepted 5 August 2019.

*For correspondence (email mlchye@hku.hk).

SUMMARY

As *Oryza sativa* (rice) seeds represent food for over three billion people worldwide, the identification of genes that enhance grain size and composition is much desired. Past reports have indicated that *Arabidopsis thaliana* acyl-CoA-binding proteins (ACBPs) are important in seed development but did not affect seed size. Herein, rice OsACBP2 was demonstrated not only to play a role in seed development and germination, but also to influence grain size. *OsACBP2* mRNA accumulated in embryos and endosperm of germinating seeds in qRT-PCR analysis, while β-glucuronidase (GUS) assays on *OsACBP2pro::GUS* rice transformants showed GUS expression in embryos, as well as the scutellum and aleurone layer of germinating seeds. Deletion analysis of the *OsACBP2* 5′-flanking region revealed five copies of the seed *cis*-element, Skn-l-like motif (−1486/−1482, −956/−952, −939/−935, −826/−822, and −766/−762), and the removal of any adversely affected expression in seeds, thereby providing a molecular basis for *OsACBP2* expression in seeds. When *OsACBP2* function was investigated using *osacbp2* mutants and transgenic rice overexpressing OsACBP2 (OsACBP2-OE), *osacbp2* was retarded in germination, while OsACBP2-OEs performed better than the wild-type and vector-transformed controls, in germination, seedling growth, grain size and grain weight. Transmission electron microscopy of OsACBP2-OE mature seeds revealed an accumulation of oil bodies in the scutellum cells, while confocal laser scanning microscopy indicated oil accumulation in OsACBP2-OE aleurone tissues. Correspondingly, OsACBP2-OE seeds showed gain in triacylglycerols and long-chain fatty acids over the vector-transformed control. As dietary rice bran contains beneficial bioactive components, OsACBP2 appears to be a promising candidate for enriching seed nutritional value.

Keywords: aleurone layer, lipid profiling, oil body, *Oryza sativa*, scutellum, Skn-l-like motif.

INTRODUCTION

Rice is considered the most important food crop (Khush, 2013), acting as daily subsistence for more than three billion people globally (Elert, 2014; Woolston, 2014). Of the cereals, rice production is second to maize (Ray *et al.*, 2013) with ~162 million hectares cultivated in 2017 (FAO.ORG, 2018a), and over 43 million tons traded worldwide in 2016/2017 (FAO.ORG, 2018b). Despite a rise (130%) in rice production from 1966 to 2000 (Khush, 2005), output must accelerate to 852 million tons by 2035 to keep pace with the growing global population (Khush, 2013). To this end, genes that can improve grain yield and size of this staple crop have been intensively sought (Song *et al.*, 2007; Shomura *et al.*, 2008; Mao *et al.*, 2010; Li *et al.*, 2011; Wang *et al.*, 2015a,b; Montesinos *et al.*, 2016; Liu *et al.*, 2017).

Examples of rice genes that influence grain weight are *GRAIN WIDTH ON CHROMOSOME 2* (*GW2*), *GRAIN SIZE ON CHROMOSOME 3* (*GS3*), *GW5,* rice *BRASSINAZOLE-RESISTANT1* (*OsBZR1*), and *D11* (Song *et al.*, 2007; Shomura *et al.*, 2008; Mao *et al.*, 2010; Zhu *et al.*, 2015; Liu *et al.*, 2017). GW2, a RING-type protein with E3 ubiquitin ligase activity, affects grain width, length, and weight by regulating the development of other tissues or organs (Song *et al.*, 2007). A near isogenic line (NIL), NIL(*GW2*), enhanced grain width (26.2%), thickness (10.5%), and length (6.6%) (Song *et al.*, 2007). In contrast, grain length was negatively regulated by GS3, which contains a plant-specific organ size regulation domain (Mao *et al.*, 2010). Although transgenic rice overexpressing *GS3* showed

wider grain width (~10%), grains became shorter (~20%), culminating in reduction (~30%) in weight (Mao *et al.*, 2010).

Brassinosteroids (BRs) are essential in rice seed development, because BR-deficient mutants form short seeds (Hong *et al.*, 2005; Tanabe *et al.*, 2005; Morinaka *et al.*, 2006; Fang *et al.*, 2016; Yuan *et al.*, 2017). Furthermore, BR was found to promote grain size by stimulating cell expansion in spikelet hulls (Hong *et al.*, 2005; Yuan *et al.*, 2017; Zhou *et al.*, 2017). The GW5 protein physically interacts with rice GLYCOGEN SYNTHASE KINASE2, to downregulate BR biosynthesis (Liu *et al.*, 2017). Consequently, grain width increased (~30%) in *GW5* knockout lines, while grain weight rose (~20%) in the *GW5* deletion lines (Shomura *et al.*, 2008; Liu *et al.*, 2017). Furthermore, the overexpression of a BR-signaling factor, OsBZR1, improved grain width (6.6%), length (4.3%), and weight (3.4%), while *OsBZR1*-RNAi rice seeds had shorter grain length (7.5%), accompanied by slight reduction in grain thickness (2.1%), width (1.7%), and weight (4.4%) (Zhu *et al.*, 2015). Also, transgenic rice overexpressing the rice *D11*-encoded cytochrome P450 involved in BR biosynthesis displayed increase in grain width (9.7%), length (12.6%), and weight (7.0%), while *D11*-RNAi lines were reduced in grain weight (6.8%) and length (14.1%) (Zhu *et al.*, 2015).

Rice genes that affect grain length or width, but not weight, include *GRAIN LENGTH ON CHROMOSOME 7* (*GL7*), *SMALL AND ROUND SEED5 (SRS5),* rice *SQUAMOSA PROMOTER BINDING PROTEIN-LIKE13* (*OsSPL13*), and *GS5* (Li *et al.*, 2011; Wang *et al.*, 2015a,b; Si *et al.*, 2016). In transgenic rice, the overexpression of GL7 which interacts with OsSPL16 (GW8) in regulating grain size (Wang *et al.*, 2015a), promoted the formation of densely packed starch granules, affecting microtubule arrangement and enhancing grain length (Wang *et al.*, 2015b). In contrast, grain length declined in the *srs5* mutant which was retarded in cell elongation (Segami *et al.*, 2012). Another gene, *GS5*, encoding a putative serine carboxypeptidase, has been proposed to act as a positive modulator upstream of cell cycle genes to promote mitotic division, increasing cell number and grain width (~10%) (Li *et al.*, 2011).

Besides genes involved in regulating organ size, BR biosynthesis, cell cycles and cell elongation, we report herein that a gene encoding an acyl-CoA-binding protein (ACBP) essential for lipid metabolism can affect seed size. During rice grain development, fatty acids (FAs) accumulate as triacylglycerols (TAGs) which represent the principle energy reserve in the embryo (Clarke *et al.*, 1983). FAs must be thioesterified to Coenzyme-A derivatives by acyl-CoA synthase before they can be used as a fuel or as precursors in the biosynthesis of other lipids (Ohlrogge and Browse, 1995). ACBPs bind acyl-CoA esters to maintain an intracellular acyl-CoA pool as well as transport acyl-CoAs in lipid metabolism (Xiao and Chye, 2011; Du *et al.*, 2016; Lung and Chye, 2016c; Ye and Chye, 2016). These proteins have been reported in the plant kingdom (Meng *et al.*, 2011), other eukaryotes, and 11 eubacterial species (Burton *et al.*, 2005). *Arabidopsis thaliana* mutants lacking ACBPs showed altered lipid composition, thereby increasing stress susceptibility (Chye *et al.*, 1999; Chen *et al.*, 2008; Xiao *et al.*, 2010; Du *et al.*, 2013a,b; Xue *et al.*, 2014), retarding pollen development (Hsiao *et al.*, 2015), reducing seed weight (Hsiao *et al.*, 2014a), and causing embryonic lethality (Chen *et al.*, 2010). ACBP mutations also adversely affected embryogenesis in mammals (Zhou *et al.*, 2007; Landrock *et al.*, 2010), worms (Elle *et al.*, 2011), and insects (Majerowicz *et al.*, 2016).

In each of rice and Arabidopsis, six ACBPs co-exist in four classes (Meng *et al.*, 2011). Class I ACBPs (10 kDa) consist of only a single acyl-CoA-binding (ACB) domain (Meng *et al.*, 2011) and include rice OsACBP1, OsACBP2, and OsACBP3 and Arabidopsis AtACBP6 (Meng *et al.*, 2011). Arabidopsis Class II ACBPs [AtACBP1 (Li and Chye, 2003), and AtACBP2 (Li and Chye, 2003; Gao *et al.*, 2009, 2010)] are characterized by a transmembrane domain and an ankyrin-repeat domain. Knockout of *AtACBP1* increased C18:0-CoA, monogalactosyldiacylglycerol (MGDG), and polyunsaturated fatty acids (PUFA) content at the expense of phosphatidylcholines (PC), phosphatidylinositol (PI), and phosphatidylserine (PS) in siliques, reduced epicuticular wax crystals and increased susceptibility to *Botrytis cinerea* (Chye *et al.*, 1999; Chen *et al.*, 2010; Du *et al.*, 2013a; Xue *et al.*, 2014). Furthermore, the *atacbp1atacbp2* double mutant was embryo lethal (Chen *et al.*, 2010). AtACBP4 and AtACBP5 belong to Class IV and are located in cytosol, same as AtACBP6 (Meng *et al.*, 2011). Pollen abortion and reduction in seed number were evident in *atacbp4atacbp6, atacbp5atacbp6,* and *atacbp4atacbp5atacbp6* (Hsiao *et al.*, 2015). The number of seed oil bodies declined and pollen activity was impaired in *atacbp4atacbp5atacbp6* (Hsiao *et al.*, 2015).

Although ACBPs are essential in embryogenesis and seed development (Chye *et al.*, 1999; Chen *et al.*, 2010; Napier and Haslam, 2010; Hsiao *et al.*, 2014a; Lung *et al.*, 2017, 2018), a single ACBP which affects seed size and weight has not been encountered (Xiao and Chye, 2009, 2011; Du and Chye, 2013; Du *et al.*, 2016; Lung and Chye, 2016a,b,c; Ye and Chye, 2016). To better elucidate the biological role of ACBPs in rice seeds, investigations on *OsACBP2* were pertinent based on its microarray data profile (Sato *et al.*, 2010), demonstrating high *OsACBP2* expression in developing seeds.

RESULTS

OsACBP2 is highly expressed in developing and germinating rice seeds

When the temporal and spatial expression of *OsACBP2* was investigated by generating *OsACBP2pro::GUS*

transgenic rice lines for histochemical β-glucuronidase (GUS) assays, signals were observed in seed development only from 16 days after fertilization (DAF) at seed maturation (Figure 1a). The *OsACBP2* expression profile in developing seeds (Figure 1a) was consistent with microarray data from the RiceXPro (Sato *et al.*, 2010), as displayed in the heat map which also detected its high expression in leaf blades, leaf sheath, and roots (Figure S1). In contrast, *OsACBP1*,

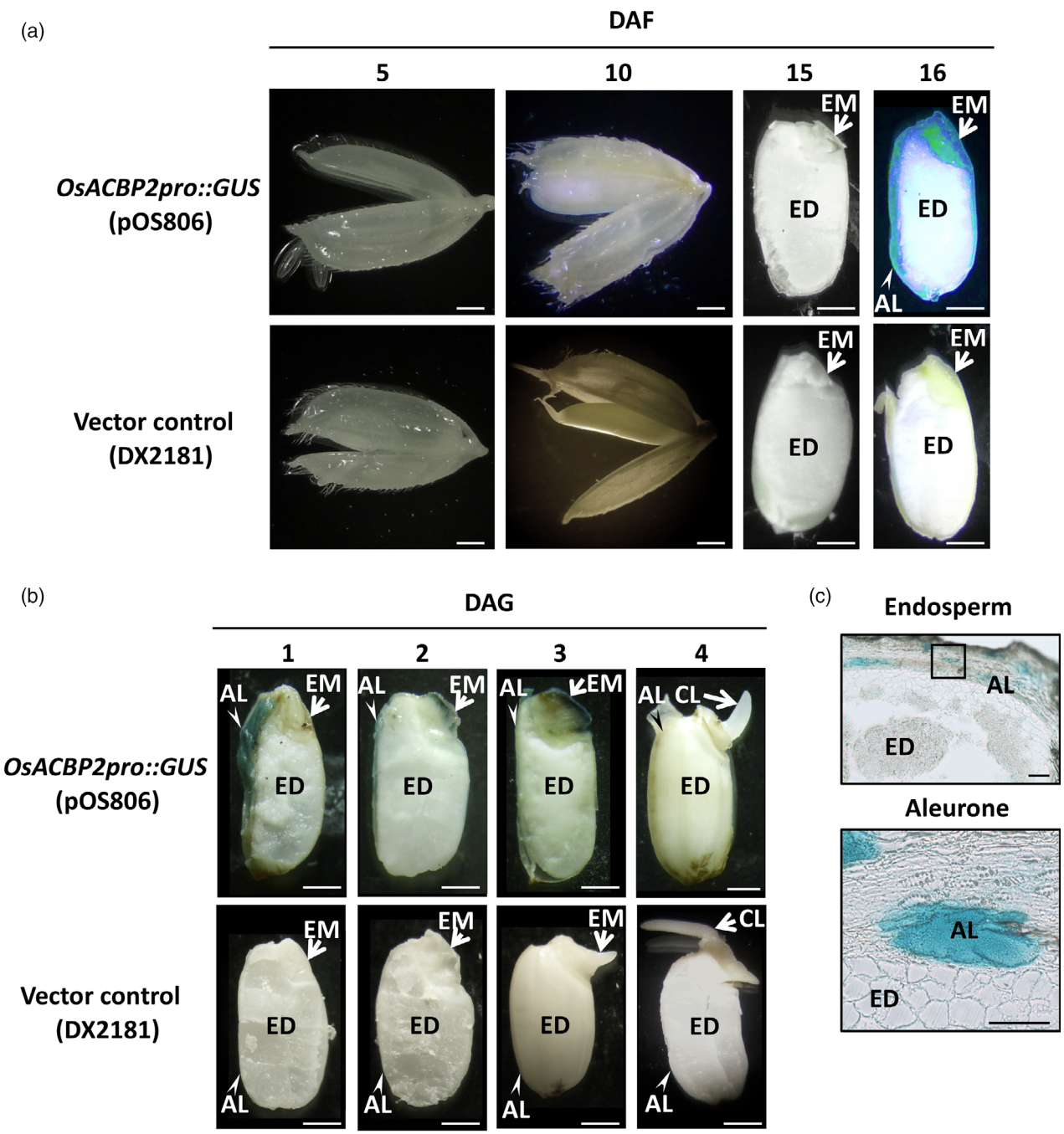

Figure 1. Examination of *OsACBP2pro::GUS* expression in developing and imbibed mature rice seeds by bright-field light microscopy.
(a) Histochemical GUS staining shows *OsACBP2pro::GUS* in longitudinally sectioned developing transgenic rice seeds 5, 10, 15, and 16 days after fertilization (DAF).
(b) Histochemical GUS staining shows *OsACBP2pro::GUS* expressions in germinating transgenic rice seeds 1, 2, 3, and 4 days after germination (DAG). GUS expression was observed in embryos (1–3 DAG) and aleurone tissue (1–2 DAG).
(c) Images of *OsACBP2pro::GUS* 1-day-old seed sections showed GUS expression in the aleurone tissue. EM, embryo; AL, aleurone; CL, coleoptile; and ED, starchy endosperm. Similar GUS expression patterns were observed in all three samples tested for each line. Bars = 1 mm in (a) and (b), and bars = 50 μm in (c).

OsACBP3, *OsACBP5*, and *OsACBP6* displayed low to moderate expression in developing seeds (Figure S1).

Furthermore, *OsACBP2pro::GUS* was highly expressed in embryos from 2 days after germination (DAG) to 3 DAG, and in aleurone from 1 to 2 DAG (Figure 1b). In 1-day-old imbibed seeds, *OsACBP2pro::GUS* was detected in the aleurone layer, but not the starchy endosperm (Figure 1c). Using qRT-PCR, *OsACBP2* was again identified to be the sole Class I *OsACBP* member highly expressed in both embryos and endosperm, 1 to 4 DAG (Figure S2). In contrast, *OsACBP1*, *OsACBP3*, *OsACBP4, OsACBP5,* and *OsACBP6* showed relatively low expression (Figure S2). In embryos, *OsACBP2* peaked at 3 DAG, with a ~4-fold increase over 1 DAG, while in the endosperm, it was highly expressed at 1 DAG and gradually declined (Figure S2), consistent with GUS staining results (Figure 1b).

Five Skn-I-like motifs regulate *OsACBP2* expression in seeds

The *OsACBP2* 5′-flanking region was predicted using PlantCARE (Lescot *et al.*, 2002) to contain five putative copies of Skn-I-like motifs, previously identified to mediate seed expression (Washida *et al.*, 1999), at nucleotide positions −1486/−1482, −956/−952, −939/−935, −826/−822, and −766/−762 (Figure 2a). Furthermore, there were four putative TGACG motifs at −1271/−1267, −1189/−1185, −339/−335, and −33/−29 (Figure 2a), which potentially recruit TGACG transcription factors in response to MeJA (Spoel *et al.*, 2003), and a putative abscisic acid-responsive (ABRE) element at −157/−147 (Figure 2a).

To verify the function of the Skn-I-like motifs, transgenic rice expressing GUS under the control of the *OsACBP2pro* and its truncated derivatives were generated (Figure 2a). Histochemical staining of 1-day-old imbibed seeds transformed with plasmids pOS806, pOS883, pOS837, pOS886, pOS859, and the DX2181 (Du *et al.*, 2010a) vector-transformed control (VC), demonstrated GUS expression in all lines except pOS859 and VC transformants (Figure 2b). Interestingly, only pOS806 transformants with all five Skn-I-like motifs (−1486/−1482, −956/−952, −939/−935, −826/−822, and −766/−762) displayed GUS expression in both endosperm and embryos (Figure 2b). In contrast, GUS signals in pOS883 transformants with four Skn-I-life motifs (−956/−952, −939/−935, −826/−822, and −766/−722), pOS837 transformants with two Skn-I-life motifs (−826/−822 and −766/−722), and pOS886 transformants with one Skn-I-life motif (−766/−722) were embryo-specific (Figure 2b). Removal of the Skn-I-like motifs at −956/−952 and −939/−935 (pOS837) drastically diminished GUS activity in transgenic rice *OsACBP2pro::GUS* seeds, while removal of the remaining Skn-I-like motifs at −826/−822 and −766/−762 (pOS859) further reduced GUS activity (Figure 2b). This reduction in GUS signal observed with the sequential removal of Skn-I-like motifs from the *OsACBP2* 5′-flanking region (Figure 2) correlated well with GUS histochemical stains (Figure 1).

To further investigate the function of the putative Skn-I-like motifs in the *OsACBP2* 5′-flanking region, electrophoretic mobility shift assays (EMSAs) were performed using double-stranded biotin-labeled DNA probes containing the five Skn-I-like motifs (−1486/−1482, −956/−952, −939/−935, −826/−822, and −766/−762). When crude nuclear extracts from 1-day-old imbibed seeds were tested, band shifts occurred with all four sets of probes, indicating DNA–protein interaction (Figure 2d). In contrast, the use of 200-fold non-biotin-labeled mutagenized probe for each Skn-I-like motif (−1486/−1482, −956/−952, −939/−935, −826/−822, and −766/−762), with substitution of 'GTCAT' to 'GGCCC' (Figure 2c) failed to outcompete protein binding in this loss-of function study (Figure 2d). However, binding was outcompeted in the presence of 200-fold non-biotin-labeled wild-type probe for each Skn-I-like motif (Figure S3), suggesting that all five Skn-I-like motifs interact with nuclear proteins.

OsACBP2 overexpression enhances grain size and weight in transgenic rice

To study OsACBP2 function, an *osacbp2* T-DNA insertional mutant PFG_1D-05815 (*osacbp2*-P05815) from the Rice T-DNA Insertion Sequence Database (RISD DB, cbi.khu.ac.kr/

Figure 2. Regulation of *OsACBP2* expression by Skn-I-like motifs in imbibed mature rice seeds.
(a) Schematic diagram of *OsACBP2pro::GUS* constructs in which the *OsACBP2* 5′-flanking sequence was fused to the *GUS* reporter gene. Putative *cis*-elements on the *OsACBP2* 5′-flanking region (pOS806) and its deletion derivatives (pOS883, pOS837, pOS886 and pOS859) are presented by blue rectangles (Skn-I-like motifs), gray triangles (TGACG motifs), and orange ovals (ABRE motifs). The plasmid DX2181 was used as a vector control. Skn-I, Skn-I-like motif; TGACG, TGACG motif-binding factor; ABRE, abscisic acid-responsive element; GUS, β-glucuronidase. The putative Skn-I-like motifs were located at −1486/−1482, −956/−952 and −939/−935, −826/−822 and −766/−762. The putative TGACG motifs (−1271/−1267, −1189/−1185, −339/−335, and −33/−29) and putative ABRE (−157/−147) are marked.
(b) GUS assays on 1-day-old imbibed seeds from transgenic ZH11 *OsACBP2pro::GUS* rice transformants of pOS806 and its deletion derivatives (pOS883, pOS837, pOS886 and pOS859). The DX2181 transformant was used as a vector control. Quantitative fluorometric measurement was obtained from experiments performed with five independent lines for each construct, and 10 seeds per line were used for GUS extraction. Bars indicate the standard errors of three replicates. Asterisks indicate significantly higher ($P < 0.05$ using Student's *t*-test) GUS activity than the DX2181 vector-transformed control. Arrowheads indicate GUS signals. Bars = 1 mm.
(c) Schematic illustration of five mutated Skn-I-like motifs (−1486/−1482, −956/−952, −939/−935, −826/−822, and −766/−762) and their corresponding locations in the Skn-I-like motif wild-type probe sequences. Mutated nucleotides in Skn-I-like motifs and their corresponding sequences are bolded.
(d) Electrophoretic mobility shift assays show binding of nuclear extracts to the Skn-I-like motifs in the *OsACBP2* 5′-flanking region. The competitor contains 200× non-biotin-labeled mutagenized probe shown in (c). -, absent in the reaction; +, present in the reaction. Arrowheads indicate DNA–protein binding complexes formed in the presence of nuclear proteins extracted from 1-day-old imbibed rice seeds. Arrow indicates free unbound biotin-labeled probe. In contrast, 200× non-biotin-labeled wild-type probes competed out the biotin-labeled probes (Figure S3).

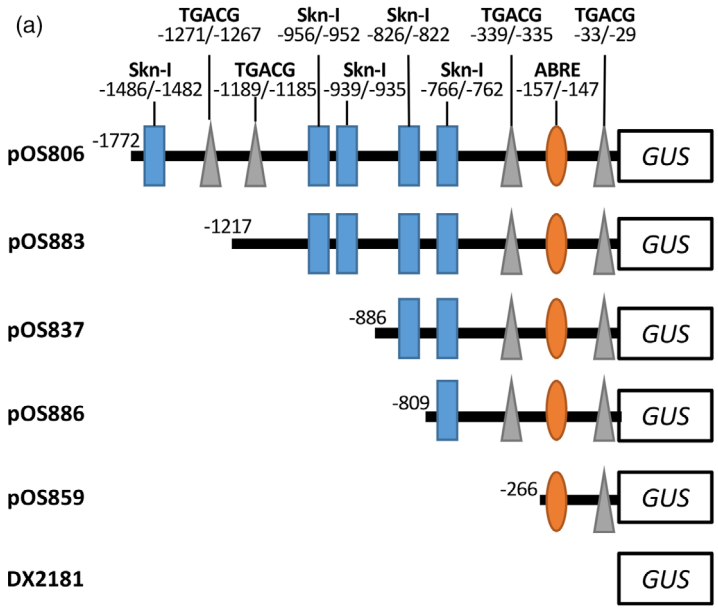

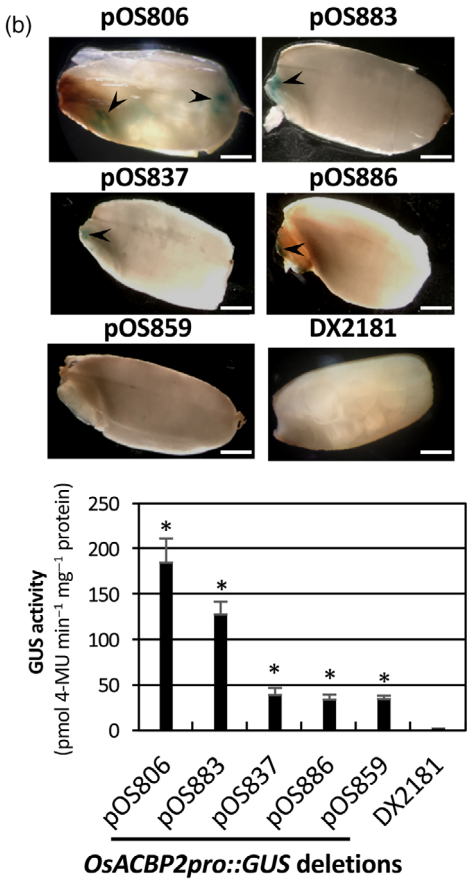

(c)

Skn-I-(-1486/-1482)-wt
TCCTTTTAT**GTCAT**TTGCGCTGATGTACA
AGGAAAATA**CAGTA**AACGCGACTACATGT

Skn-I-(-1486/-1482)-mutant
TCCTTTTAT**GGCCC**TTGCGCTGATGTACA
AGGAAAATA**CCGGG**AACGCGACTACATGT

Skn-I-(-956/-952)&(-939/-935)-wt
ACCTG**GTCAT**CACATTGACAAA**ATGAC**
TGGAC**CAGTA**GTGTAACTGTTT**TACTG**

Skn-I-(-956/-952)&(-939/-935)-mutant
ACCTG**GGCCC**CACATTGACAAA**GGGCC**
TGGAC**CCGGG**GTGTAACTGTTT**CCCGG**

Skn-I-(-826/-822)-wt
ATAGCCTCAGTTTGTTT**GTCAT**CCCTATAT
TATCGGAGTCAAACAAA**CAGTA**GGGATATA

Skn-I-(-826/-822)-mutant
ATAGCCTCAGTTTGTTT**GGCCC**CCCTATAT
TATCGGAGTCAAACAAA**CCGGG**GGGATATA

Skn-I-(-766/-762)-wt
ACGAGAT**GTCAT**CCTGTACTGTCCATGTT
TGCTCTA**CAGTA**GGACATGACAGGTACAA

Skn-I-(-766/-762)-mutant
ACGAGAT**GGCCC**CCTGTACTGTCCATGTT
TGCTCTA**CCGGG**GGACATGACAGGTACAA

(d)

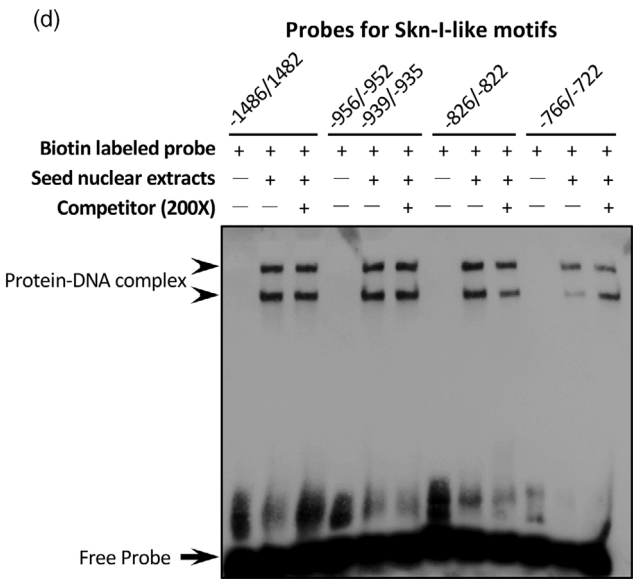

RISD_DB.html) and three retrotransposon insertional mutants RMD_03Z11AZ19 (*osacbp2*-AZ19), RMD_03Z11LE18 (*osacbp2*-LE18), and RMD_03Z11LG76 (*osacbp2*-LG76) of *OsACBP2* from the Rice Mutant Database (RMD, rmd.ncpgr.cn) were characterized (Figure S4a). The *osacbp2*-P05815 mutant was derived from the Hwayoung wild-type

(HY), and its T-DNA insertion was mapped to the 5′-untranslated region (UTR) (Figure S4a). The *osacbp2* mutants, *osacbp2*-AZ19, *osacbp2*-LE18, and *osacbp2*-LG76 originated from the Zhonghua11 wild-type (ZH11). The inserts were localized at the 3′-UTR for *osacbp2*-LE18 and *osacbp2*-LG76, while the insert for *osacbp2*-AZ19 was mapped to the third exon (Figure S4a).

As OsACBP2 shares 79% amino acid identity with OsACBP1 (Guo *et al.*, 2017), anti-OsACBP1 antibodies were found to cross-react with recombinant OsACBP2 (Figure S4b). Western blot analysis with anti-OsACBP1 antibodies using 1-day-old rice seeds confirmed OsACBP2 expression was significantly impaired in all four lines (*osacbp2*-AZ19, *osacbp2*-LE18, *osacbp2*-LG76 and *osacbp2*-P05815; Figure S4c and d). The *osacbp2* seeds did not show *OsACBP2* mRNA expression at 1–4 DAG (Figure S4e). Seed germination and seedling growth were retarded in *osacbp2*-P05815 from 2 DAG, while *osacbp2*-P05815 seeds at 4 DAG did not possess the elongated coleoptiles evident in the wild-type (WT) (at 3–4 DAG) (Figure S4f). Germination tests revealed that OsACBP2-OEs germinated more rapidly than the WT and VC, while *osacbp2* germination was slower (Figure S5). At 4 DAI, the germination rate of OsACBP2-OEs was higher than the VC, while fewer germinated seeds appeared for *osacbp2* than the corresponding control (Figure S5).

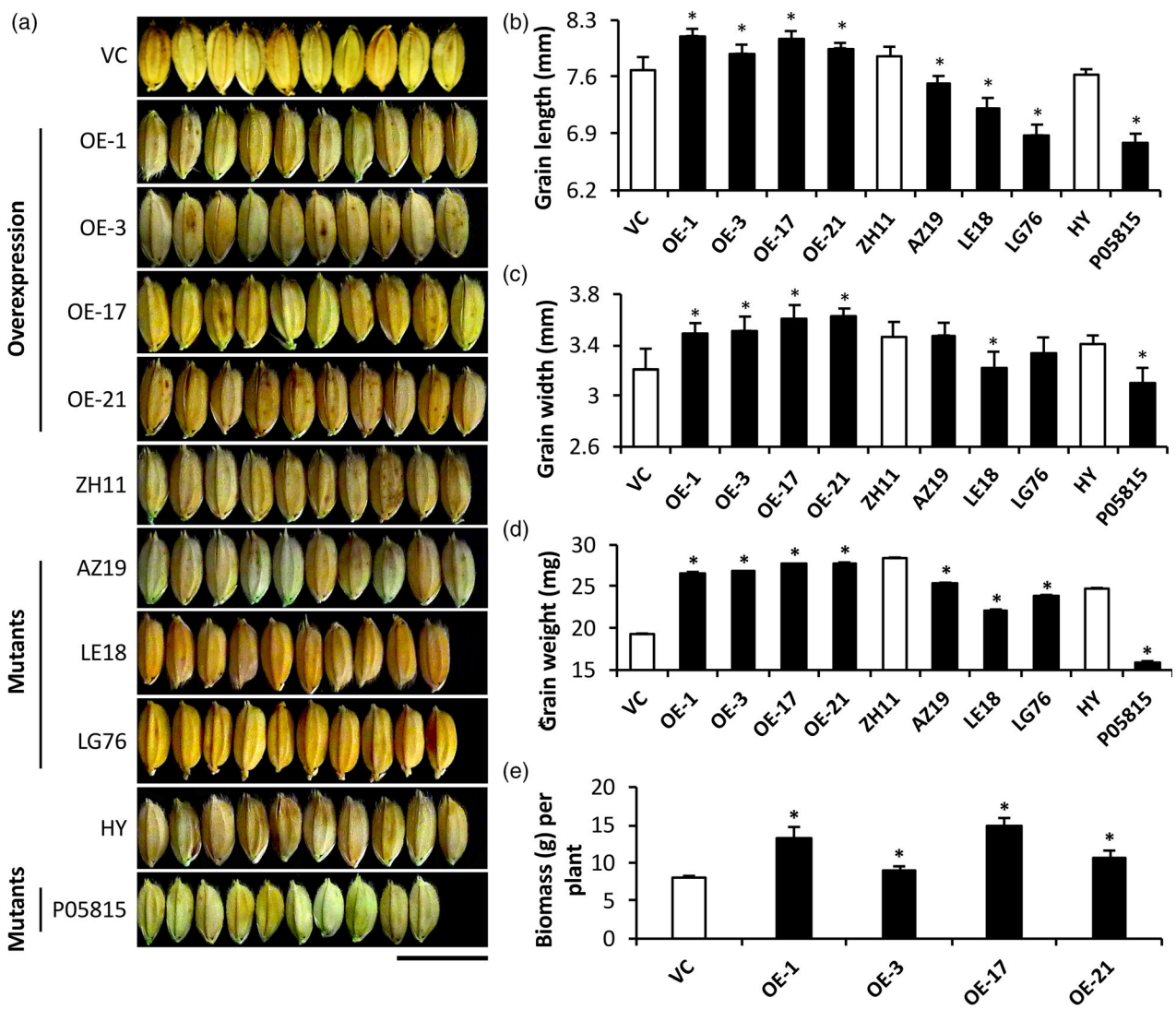

Figure 3. Measurement of seed length, width and weight in OsACBP2-OEs and *osacbp2* mutants.
(a) Grains from pCXSN vector control (VC), OsACBP2-OEs (OE-1, OE-3, OE-17, and OE-21), Zhonghua11 wild-type (ZH11), *osacbp2*-AZ19 (AZ19), *osacbp2*-LE18 (LE18), *osacbp2*-LG76 (LG76), Hwayoung wild-type (HY), and *osacbp2*-P05815 (P05815). The background for *osacbp2*-AZ19, *osacbp2*-LE18 and *osacbp2*-LG76 is ZH11, while that for *osacbp2*-P05815 is HY. Bar = 10 mm. Comparison in grain length (b), grain width (c), grain weight (d), and biomass per plant (e) amongst the OsACBP2-OEs, controls (VC, ZH11, and HY), and *osacbp2* mutants [$n = 30$, and $n \geq 5$ for (e)]. The values in (b–e) represent the mean ± SE. Asterisks indicate significant differences ($P < 0.05$ using Student's *t*-test) from relevant controls.

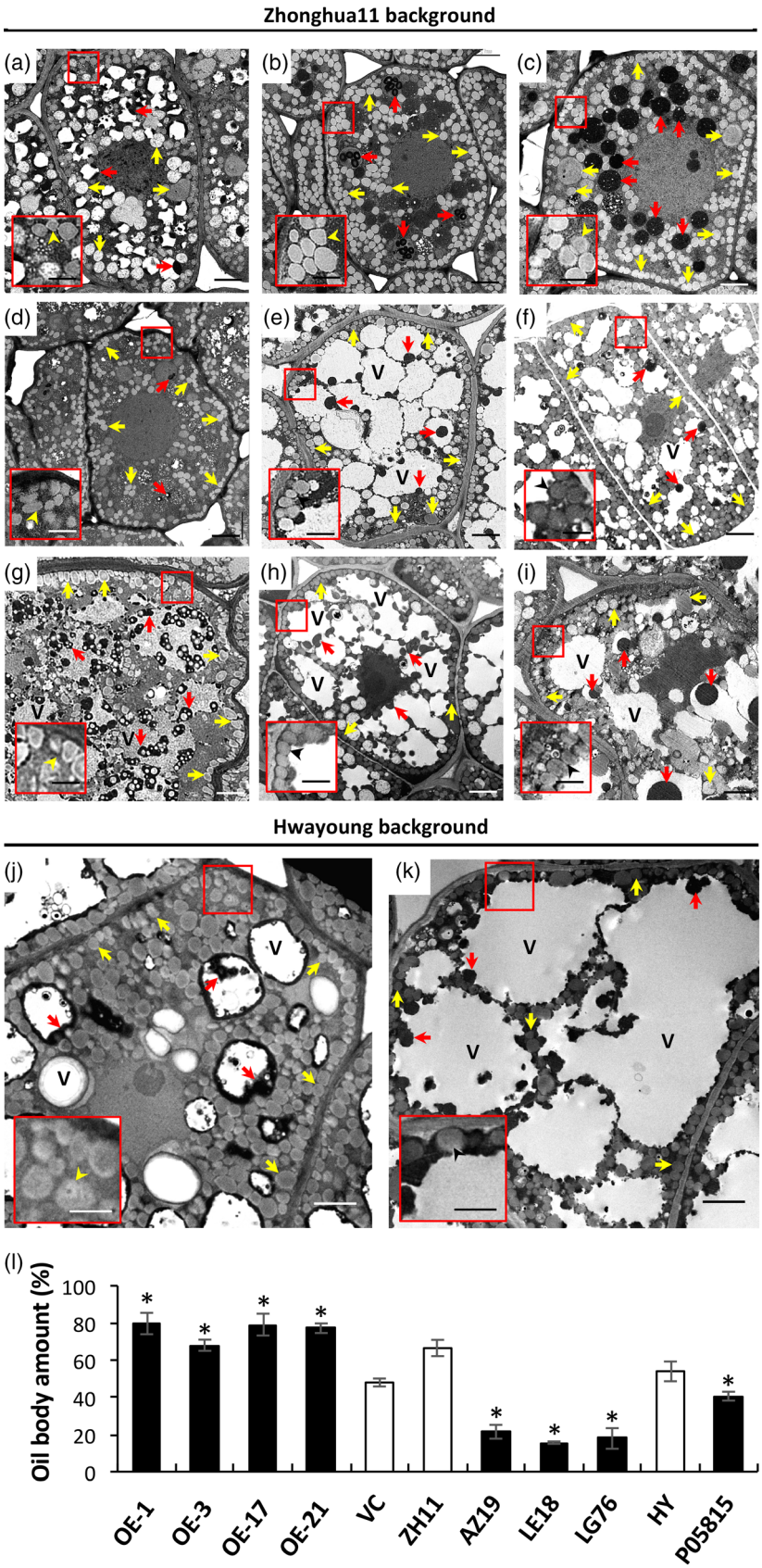

Figure 4. Transmission electron microscopy of the scutellum cells from imbibed rice seeds from OsACBP2-OEs and *osacbp2*.Scutellum cells of OsACBP2-OEs, OE-1 (a), OE-3 (b), OE-17 (c), and OE-21 (d), showed increase in oil bodies (yellow arrows) and protein bodies (red arrows) in comparison with the pCXSN vector control (e). Scutellum cells in the *osacbp2* mutant lines *osacbp2*-AZ19 (g), *osacbp2*-LE18 (h), *osacbp2*-LG76 (i) contained fewer oil bodies in comparison with ZH11 (f), and *osacbp2*-P05815 (k) fewer than Hwayoung wild-type (j). 'V' indicates vacuoles. Oil bodies in the boxed areas are magnified in the insets. Bars = 2 μm and 0.8 μm (inset). (l) Percentage area of oil bodies in a single scutellum cell was measured using ImageJ software. Values indicate mean ± SE (n = 3). Asterisks indicate significantly more oil bodies than the pCXSN vector-transformed control. Asterisks indicate significantly higher ($P < 0.05$ using Student's t-test) intensity in comparison with the pCXSN vector-transformed control.

When seed characteristics were examined, transgenic rice OsACBP2-OEs displayed improved grain length (+10%), width (+10%), and weight (+10%), in comparison with the VC (Figure 3). Correspondingly, the four *osacbp2* lines (*osacbp2*-P05815, *osacbp2*-AZ19, *osacbp2*-LE18, and *osacbp2*-LG76) exhibited reduction in grain length (−5%) and weight (−10%) in comparison with their corresponding WTs (Figure 3). Besides, seeds from two mutant lines, *osacbp2*-LE18 and *osacbp2*-P05815, were narrower than their corresponding WTs (Figure 3c). Consequently, the grain yield biomass of each OsACBP2-OE line exceeded the VC (Figure 3e). When 2-week-old wild-type controls (ZH11 and HY), the VC (pCXSN), *osacbp2* mutants (*osacbp2*-AZ19, *osacbp2*-LE18, *osacbp2*-LG76 and *osacbp2*-P05815) and OsACBP2-OEs (OE-1, OE-3, OE-17, and OE-21) were compared, OsACBP2-OEs showed higher coleoptile and shoot elongation rates than ZH11 and the VC (Figure S6b). Mutants were reduced in both shoot and coleoptile elongation rates in comparison with their corresponding WTs (Figure S6b). Nonetheless, the mature plant height of 49-day-old OsACBP2-OE was not greater than the controls (Figure S6c).

OsACBP2-OE transgenic rice seeds accumulate storage lipids

To investigate how OsACBP2 confers increase in grain size and weight, the scutellum cells from transgenic OsACBP2-OE rice seeds were examined using transmission electron microscopy (TEM). Resembling the oil body distribution characteristic for oil seeds (Mansfield and Briarty, 1992; Siloto *et al.*, 2006), oil bodies in the rice scutellum appeared as discrete regularly sized organelles under TEM (Figure 4). They were present at the periphery of the cells and between protein bodies (Figure 4). The different intracellular structures of scutellum cells amongst OsACBP2-OEs or *osacbp2* may have arisen from their varying rates in nutrient breakdown, resulting in differences in germination rate (Figures S5, S6a and b). More oil bodies were encountered in the OsACBP2-OEs (Figure 4a–d) than the VC (Figure 4e) and ZH11 (Figure 4f). Fewer oil bodies were detected in the *osacbp2* mutants in both ZH11 and HY backgrounds: *osacbp2*-AZ19 (Figure 4g), *osacbp2*-LE18 (Figure 4h), and *osacbp2*-LG76 (Figure 4i) in comparison with ZH11 (Figure 4f), and *osacbp2*-P05815 (Figure 4k) to HY (Figure 4j). Quantitative analysis on lipid bodies using ImageJ confirmed that OsACBP2-OEs possessed more oil bodies than the VC (Figure 4l), and analysis on Nile red-stained aleurone cells showed that more oil accumulated in OsACBP2-OE aleurone than the VC (Figure 5). In contrast, the *osacbp2* aleurone contained less oil than its corresponding control (Figure S7).

Electrospray ionization mass spectrometry (ESI-MS) analysis revealed that the total amount of TAGs in OsACBP2-OE seeds was greater than the VC and ZH11

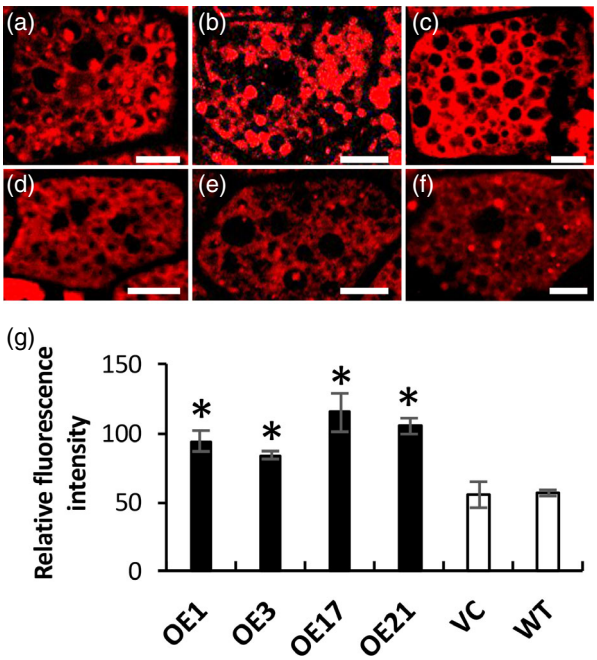

Figure 5. Confocal laser scanning microscopy of the OsACBP2-OE aleurone cells from Nile red-stained imbibed rice seeds.
Aleurone cells of OsACBP2-OEs, OE-1 (a), OE-3 (b), OE-17 (c), and OE-21 (d) showed stronger fluorescence intensity in comparison with the pCXSN vector control (VC) (e) and Zhonghua11 wild-type (WT) (f). Bars = 10 μm. (g) Oil content of OsACBP2-OE aleurone cells. Relative fluorescence intensity was measured using ImageJ on Nile red-stained OsACBP2-OE aleurone cells. Asterisks indicate significantly higher ($P < 0.05$) using Student's *t*-test) intensity than the pCXSN vector-transformed control.

(Figure 6; Table S1). Unsaturated TAGs (50:2-, 52:2-, 52:4-, and 54:2-TAG) increased in OsACBP2-OEs over the VC (Figure 6; Table S1). Using gas chromatography–mass spectrometry (GC-MS), the total FA content in OsACBP2-OE seeds was ~10% higher than the VC, while *osacbp2*-P05815 and *osacbp2*-LE18 seeds showed 10–20% decrease in total FA content (Table S2). Also, C18:0-FA accumulated in the OsACBP2-OEs over the VC (Table S2). Subsequently OsACBP2-OE embryos were examined in GC-MS to estimate the content of the ten major FA species (C14:0-, C16:0-, C16:1-, C18:0-, C18:1-, C18:2-, C18:3-, C20:0-, C20:1-, and C22:0-FA), among which the three most abundant ones (totaling > 90%) were C16:0-FA (20–24%), C18:1-FA (32–37%), and C18:2-FA (32–37%) (Figure 7). C18:1-FA was higher in three OsACBP2-OE lines (OE-1, OE-3, and OE-17), while C18:2-FA was higher in OsACBP2-OE-1, OE-3, and OE-21 (Figure 7). Furthermore, statistically significant increase in C16:0- and C22:0-FA was detected in OsACBP-OEs over the control (Figure 7). Also, many other FAs, both saturated (C14:0-, C18:0-, and C20:0-FAs) and unsaturated (C18:3- and C20:1-FAs) FA constituents showed different accumulation patterns in the overexpression lines (Figure 7). These results demonstrated that the OsACBP2-OEs over-accumulated long-chain FAs (LCFAs) in mature embryos (Figure 7).

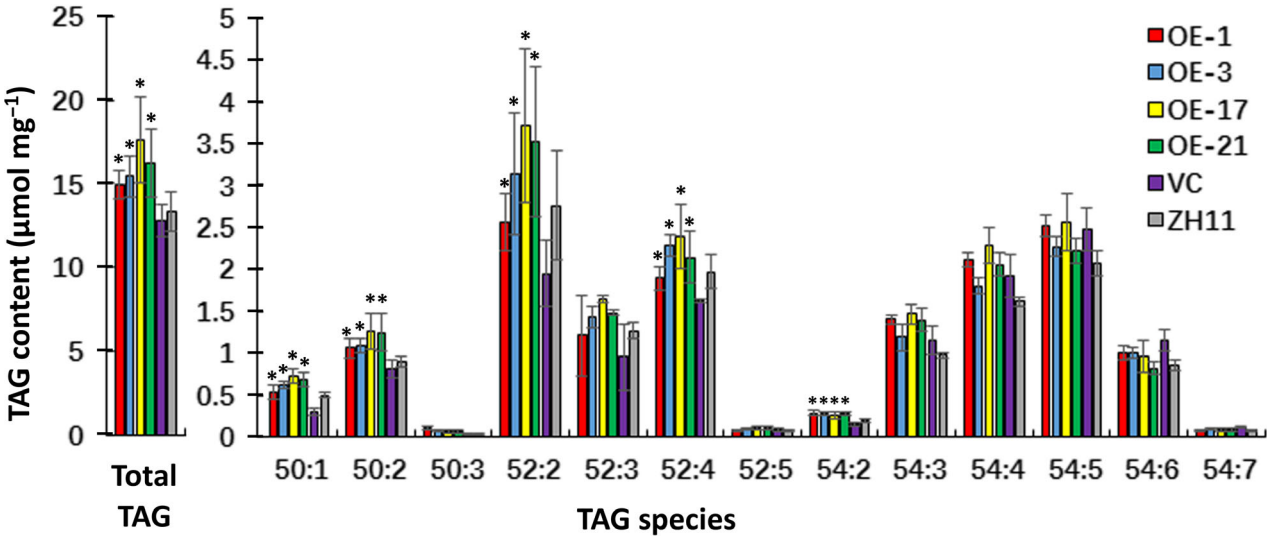

Figure 6. Analysis of fatty acid content and composition in OsACBP2-OEs.
Quantitative analysis of triacylglycerols (TAGs; C50:1, C50:2, C50:3, C52:2, C52:3, C52:4, C52:5, C54:2, C54:3, C54:4, C54:5, C54:6, and C54:7) from 1-day-old imbibed rice seeds OsACBP2-OEs, OE-1 (red), OE-3 (blue), OE-17 (yellow), OE-21 (green), pCXSN vector-transformed control (purple) and ZH11 wild-type (gray). Values are mean ± SE of measurements made on three independent batches of samples (n = 20). Asterisks indicate significantly higher value in comparison with the VC using Student's t-test ($P < 0.05$).

Figure 7. Gas chromatography–mass spectrometry analysis of fatty acids from OsACBP2-OE transgenic rice embryos.Quantitative analysis of fatty acids (C14:0, C16:0, C16:1, C18:0, C18:1, C18:2, C18:3, C20:0, C20:1 and C22:0-FA) from embryos of rice OsACBP2-OEs, OE-1 (red), OE-3 (blue), OE-17 (yellow), OE-21 (green), pCXSN vector-transformed control (purple) and ZH11 wild-type (gray). Values represent mean ± SE of measurements made on three independent batches of samples. Student's t-test was performed on each OsACBP2-OE against VC. Asterisks indicate significantly higher value ($P < 0.05$). Each measurement contains 40 seeds.

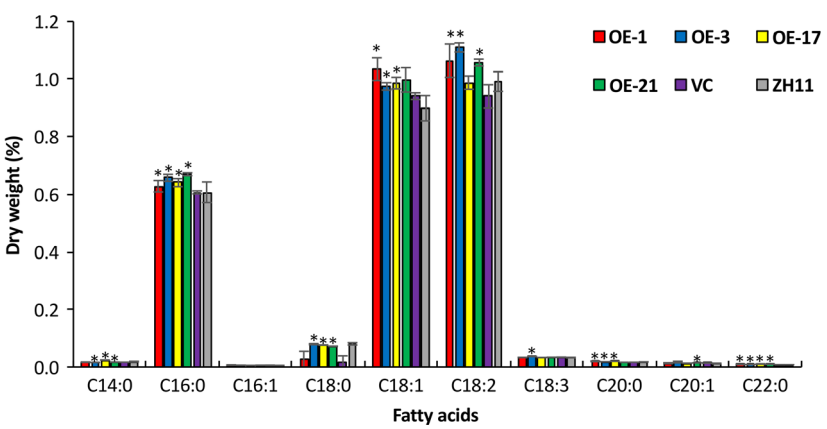

DISCUSSION

High *OsACBP2* expression in rice seeds is regulated by Skn-l-like motifs

Of the six *OsACBPs* verified in qRT-PCR analysis to show different expression profiles during seed germination (Figure S2), *OsACBP2* was the most highly expressed in germinating seeds (Figure S2), consistent with the microarray data (Figure S1) and previous qRT-PCR results on high *OsACBP2* expression in milk and soft dough seeds (Meng *et al.*, 2011). Its high seed expression was related to the presence of two adjacent (−956/−952 and −939/−935) Skn-l-like motifs in its 5′-flanking region (Figure 2a), as confirmed by EMSAs to effectively bind nuclear proteins (Figures 2d and S3). Skn-1 was first reported in *Caenorhabditis elegans* as a transcription factor to determine the cell fate in the early embryo (Bowerman *et al.*, 1992) and play a role in oxidative responses (An and Blackwell, 2003). EMSAs demonstrated that Skn-l recognizes 'GTCAT' and 'ATCAT' DNA sequences (Blackwell *et al.*, 1994). Similar motifs in the 5′-flanking regions of plant genes, designated as Skn-l-like motifs, are known to regulate seed-specific expression (Washida *et al.*, 1999). These motifs are enriched in the 5′-flanking region of the gene encoding the Poaceae seed storage protein (SSP) (Fauteux and Stromvik, 2009). However, genes regulated by Skn-l-like motifs, such as *Poaceae SSP* and the rice storage protein glutelin gene *GluB-1* (Washida *et al.*, 1999), have not been previously associated with grain size and weight.

OsACBP2 plays a role in seed storage because its high expression in developing seeds at 16 DAF (Figure 1a) coincided with the accumulation of rice storage compounds such as starches, proteins and lipids (Deng *et al.*, 2013). This role was further supported by its high expression in

germinating rice seeds (GUS assays in Figure 1b), while *osacbp2* seeds were retarded in germination (Figure S6b). As TEM and confocal microscopy showed fewer oil body accumulation in *osacbp2* embryo and aleurone cells (Figures 4 and 5), OsACBP2 appeared to participate in oil accumulation during seed development. Besides lipids, sugars represent another essential nutrient for rice seed development (Halford and Paul, 2003). Interestingly, knockout mutants of rice *SnRK1*, which encodes the SNF1-RELATED PROTEIN KINASE1, were impaired in sugar signaling and retarded in seed germination (Lu *et al.*, 2007).

OsACBP2 affects seed TAG content

In this study, TAG (50:1-, 50:2-, 52:2-, 52:4-, and 54:2-TAGs) and FA (C14:0-, C16:0-, C18:0-, C18:1-, C20:0-, and C22:0-FAs) accumulation in OsACBP2-OE seeds (Figures 6 and 7) resulted in gain in OsACBP2-OE grain size and weight over the VC (Figure 3). In plant seeds, TAGs, in the form of oil bodies, represent a crucial energy reserve during germination (Murphy, 1994; Chapman *et al.*, 2012; Hernández *et al.*, 2012; Pyc *et al.*, 2017), and they constitute a major component of seed oil (reviewed in Weselake *et al.* (2009)). FAs need to be converted to CoA esters before TAG biosynthesis via the Kennedy pathway (Weselake *et al.*, 2009). Thus, acyl-CoA esters (mostly C16:0 and C18:1) are the essential precursors of TAGs (Ohlrogge and Browse, 1995) and cytosolic OsACBP2 could play an important role by binding and transporting them besides maintaining an acyl-CoA pool in rice seeds.

Evidence that ACBPs bind acyl-CoA esters is based on previous observations of recombinant OsACBP2 binding to C16:0-, C18:2-, and C18:3-CoAs in isothermal titration calorimetry (Guo *et al.*, 2017). In OsACBP2, C18:3-CoA interaction occurred at a deep (depth 8–9 Å) narrow (9–10 Å) groove (Guo *et al.*, 2017), resembling the association of human liver ACBP with C14:0-CoA (Taskinen *et al.*, 2007). In contrast, OsACBP1 interacts with C16:0-CoA, similar to bovine ACBP which involves a relatively wide (width 17–18 Å) shallow (depth 4–5 Å) groove (Kragelund *et al.*, 1993). Interestingly, OsACBP1 showed stronger affinity to C16:0-CoA than C18:2- and C18:3-CoAs, perhaps due to the higher flexibility at this binding region (Guo *et al.*, 2017).

Similar to the recombinant OsACBPs, recombinant AtACBPs have also been shown to bind acyl-CoAs esters and phospholipids *in vitro* (Leung *et al.*, 2006; Chen *et al.*, 2010; Xiao *et al.*, 2010; Hsiao *et al.*, 2014a; Hu *et al.*, 2018). $(His)_6$-AtACBP1 binds PA and unsaturated PCs (18:1- and 18:2-PCs) as well as 18:2- and 18:3-CoAs, while $(His)_6$-AtACBP2 binds lysoPC, C16:0-, C18:2-, and C18:3-CoAs (Gao *et al.*, 2009, 2010; Chen *et al.*, 2010; Du *et al.*, 2013a). Besides PC, PE, and PA, $(His)_6$-AtACBP3 was reported to bind C12:0-, C14:0-, C16:0-, C16:1-, C17:0-, C18:1-, C18:2-, C18:3-, and 20:4-CoAs (Leung *et al.*, 2006; Xiao *et al.*, 2010; Hu *et al.*, 2018). Also, $(His)_6$-AtACBP4, $(His)_6$-AtACBP5, and $(His)_6$-AtACBP6 bind C14:0-, C16:0-, C18:0-, C18:1-, C18:2-, and C18:3-CoAs (Hsiao *et al.*, 2014a). Not surprisingly, transgenic Arabidopsis AtACBP-OEs showed alterations in lipid composition in comparison with the WT (Du *et al.*, 2010b, 2013a; Xiao *et al.*, 2010; Liao *et al.*, 2014). For example, PC and PA were reported to accumulate in AtACBP1-OE seeds and 5-week-old AtACBP1-OE plants in comparison with the WT (Du *et al.*, 2010b, 2013a). As PA is essential in ABA signaling, AtACBP1-OE seeds and seedlings became more sensitive to ABA treatment than the WT (Du *et al.*, 2010b, 2013a). PA also increased in AtACBP3-OEs, at expense of PC, PI, and PE (Xiao *et al.*, 2010). As PE content is crucial to cell membrane integrity, transgenic Arabidopsis AtACBP3-OE showed early leaf senescence, indicating that AtACBP3 can affect leaf lipid composition (Xiao *et al.*, 2010). Also, transgenic Arabidopsis AtACBP6-OEs displayed enhanced cold tolerance, coinciding with PC and MGDG accumulation in rosettes and flowers, suggesting that cell membrane remodelation occurred in cold-stressed AtACBP6-OEs (Liao *et al.*, 2014). In this study, the overexpression of OsACBP2, the rice homologue of AtACBP6, raised total TAG content in rice seeds (Figure 6) and promoted seed germination (Figure S5). In contrast, TAGs were not available to fuel post-germinative growth in the Arabidopsis *sdp1* mutant lacking the TAG lipase which initiates storage oil breakdown in germinating seeds, resulting in retarded seed germination (Eastmond, 2006).

Higher OsACBP2-OE seed oil content coincided with bigger grains

Besides increasing TAG content, OsACBP2 overexpression affected grain weight (Figure 6), because OsACBP2-OE transgenic rice seeds were bigger and heavier than those of the VC (Figure 3a–d). OsACBP2 overexpression in transgenic rice also culminated in enhancing grain yield (Figure 3e). Correspondingly, the *osacbp2* mutants showed lower TAG content than their respective WTs (HY and ZH11), while the OsACBP2-OEs showed elevation in unsaturated TAGs (Figure 6; Table S1) and were found to contain more LCFAs (Figure 7), implying the possible involvement of OsACBP2 in the Kennedy pathway (reviewed in Weselake *et al.* (2009)). When OsACBP2 is overexpressed, more OsACBP2 molecules can potentially participate in acyl-CoA transfer from the cytosolic pool to the endoplasmic reticulum (ER), and eventually causing TAG accumulation in oil bodies (Figures 4 and 5). The participation of OsACBP2 in long-chain acyl-CoA transfer is supported by observation in higher TAG accumulation in OsACBP-OEs than the control (Figure 6). Furthermore, lipid profiling data on TAGs and FAs (Figures 6 and 7) in OsACBP2-OEs suggested that FA biosynthesis could be enhanced in the ER, providing more unsaturated acyl-chains for TAG biosynthesis.

When the Class I Arabidopsis homologue was either knocked out or overexpressed in transgenic Arabidopsis, *atacbp6* and AtACBP6-OEs did not show significant differences from the WT in seed size (Figure S8). Also, it has been reported that seed morphology and size did not vary among the double and triple mutants of *atacbp4*, *atacbp5 and atacbp6* in comparison with the WT, although the double and triple mutant seeds were lighter than the WT (Hsiao *et al.*, 2014a). In contrast, OsACBP2 influenced both grain size and weight (Figure 3). Grain weight has also been linked to changes in seed TAG content in other studies (Jako *et al.*, 2001). The overexpression of DGAT in Arabidopsis enhanced oil content (~10%) and seed weight (~20%) (Jako *et al.*, 2001), similar to OsACBP2-OEs. Unlike OsACBP2 which increases yield by enhancing grain weight, rice VIN3-LIKE2 (OsVIL2) affected yield by suppressing cytokinin degradation, increasing grain number per panicle (Yang *et al.*, 2019). In contrast, knockdown of rice *DICER-LIKE3b* (*OsDCL3b*) that functions in gene alternative splicing in rice panicles, reduced seed setting and impaired yield (Liao *et al.*, 2019). Interestingly, unlike OsACBP2-OEs, there was no effect on grain weight in OsVIL2-OE and *OsDCL3b*-RNAi lines (Liao *et al.*, 2019; Yang *et al.*, 2019).

As OsACBP2 contributes to increasing seed oil content as well as grain size and weight in transgenic rice, it presents tremendous potential for use in the genetic engineering of rice to improve grain size and composition. After all, lipids in rice bran and germs are the undervalued by-products from rice milling (Fabian and Ju, 2011). Furthermore, dietary rice bran oil is considered to be one of the most valuable and healthy oils because it contains bioactive components that lower serum cholesterol (Rong *et al.*, 1997; Wilson *et al.*, 2007; Nagasaka *et al.*, 2011), and possesses anti-oxidation (Xu *et al.*, 2001), anti-carcinogenic (Yasukawa *et al.*, 1998), and anti-allergic inflammation activities (Akihisa *et al.*, 2000). Hence, OsACBP2 is promising not only for enhancing grain size and weight but for improving nutritional value by exhibiting 10% increases in lipid content in rice bran and whole seeds.

EXPERIMENTAL PROCEDURES

Plant materials and growth conditions

Rice (*Oryza sativa* cv Hwayoung and cv Zhonghua11) was used in this study. The mutant *osacbp2* PFG_1D-05815 was purchased from the Rice T-DNA Insertion Sequence Database (RISD DB; cbi.khu.ac.kr/RISD_DB.html), and *osacbp2* RMD_03Z11AZ19, RMD_03Z11LE18, and RMD_03Z11LG76 were purchased from the Rice Mutant Database (RMD; rmd.ncpgr.cn).

Transgenic and wild-type rice seeds were germinated in half-strength Murashige and Skoog (½MS) solid medium in a growth chamber in the dark at 28°C for 3 days, then transplanted to soil pots, and grown in greenhouse (12-h light/12-h dark cycle) at 28°C to 30°C. Buckets (radius 15 cm and height 30 cm) were filled with soil. When the plants reached maturity and grains had ripened, the plants were harvested and threshed (seeds separated from the vegetative parts).

Western blot analysis

For detection of OsACBP2 following SDS-PAGE, total plant proteins were transferred to a Hybond™-ECL™ membrane (Amersham) using a Trans-Blot®cell (Bio-Rad) according to Sambrook *et al.* (1989). After incubation in blocking buffer [5% (w/v) non-fat dried milk in TTBS buffer (20 mM Tris–HCl, pH 7.5, 500 mM NaCl, 0.05% (v/v) Tween-20)] at room temperature for 1 h, the membrane was washed 3 × 10 min with TTBS buffer and then incubated in anti-recombinant $(His)_6$-OsACBP1 antibodies [1:5000, synthesized by EzBiolab (http://www.ezbiolab.com/); OsACBP1, sharing 79% amino acid sequence identity to OsACBP2, was proven to interact with recombinant OsACBP2 (Figure S4b); (Guo *et al.*, 2017)] in blocking buffer with gentle shaking at room temperature for 2 h. The membrane was washed for 2 × 5 min with TTBS, then incubated in ECL™ anti-rabbit IgG Horseradish Peroxidase-linked whole antibody (from donkey) (1:3000, GE Healthcare) in TTBS for 1 h with gentle agitation. After incubation with anti-rabbit antibodies, the membrane was washed for 3 × 10 min in TTBS. ECL™ Western Blotting Detection Reagents (GE Healthcare) was used for detection.

RNA analysis

TRIzol reagent (Invitrogen) was used for extraction of total RNA from 0.1 g of homogenized samples. Subsequently, the total RNA was reverse-transcribed using the Superscript First-strand Synthesis System (Invitrogen) according to the manufacturer's protocol. Quantitative real-time PCR was conducted on a StepOne Plus Real-time PCR system using SYBR Green Mix (Applied Biosystems) programmed as follows: 10 min at 95°C followed by 40 cycles of 95°C (15 sec) and 56°C (1 min). For each reaction, three experimental replicates were performed with gene-specific primers (Table S3), and *Oryza sativa ACTIN* (GenBank accession number X16280) as a reference gene for normalization.

Generation of *OsACBP2pro::GUS* constructs

The *OsACBP2pro::GUS* construct consisting of a 1.7-kb 5′-flanking region, amplified by primers ML2305/ML2308 (Table S3), was generated by inserting the 1.7-kb *OsACBP2pro* fragment into a pGEM-T Easy vector (Promega), and cloning into corresponding sites on binary vector DX2181 (Du *et al.*, 2010a) to yield plasmid pOS806. DNA sequence analysis was used to verify the PCR fragment cloned. The same cloning strategies were applied in the generation of pOS806 deletion derivatives pOS883, pOS837, pOS886, and pOS859 using primer pairs ML2854/ML2308, ML2591/ML2308, ML2835/ML2308, and ML2850/ML2308, respectively (Table S3).

Figure 2a indicates the location of the *cis*-elements on the nested deletion derivatives. Each plasmid offers a different set of Skn-l-like motifs as shown. Plasmid pOS806 contains the *GUS* gene driven by a 1.7-kb (−1728 to −6) *OsACBP2* 5′-flanking sequence with all five Skn-l-life motifs (−1486/−1482, −956/−952, −939/−935, −826/−822, and −766/−762; Figure 2a). Plasmid pOS883 contains the *GUS* gene driven by a 1.2-kb (−1217 – −6) *OsACBP2* 5′-flanking sequence with four Skn-l-life motifs (−956/−952, −939/−935, −826/−822, and −766/−722; Figure 2a). Plasmid pOS837 contains the *GUS* gene driven a 0.88-kb (−886 to −6) *OsACBP2* 5′-flanking sequence with two Skn-l-life motifs (−826/−822 and −766/−722; Figure 2a). Plasmid pOS886 contains the *GUS* gene driven by a 0.8-kb (−809 to −6) *OsACBP2* 5′-flanking sequence with one Skn-l-life motif (−766/−722; Figure 2a).

Plasmid pOS859 contains the *GUS* gene driven by a 0.26-kb (−266 to −6) *OsACBP2* 5′-flanking sequence lacking in Skn-l-life motifs (Figure 2a). These constructs were sent to BioRun (http://www.biorun.net) for rice Zhonghua11 transformation.

GUS assays

Histochemical GUS assays were carried out according to Jefferson *et al*. (1987) with modifications. Plant samples were immersed and vacuum infiltrated in the GUS staining solution [100 mM sodium phosphate buffer pH 7.0, 0.1% (v/v) Triton X-100, 2 mM potassium ferricyanide, 2 mM potassium ferrocyanide, 1 mg ml^{-1} 5-bromo-4-chloro-3-indolyl-β-D-glucuronide] for 2 h, and incubated and observed over a period ranging from 3 to 16 h at 37°C. Subsequently, samples were cleared in 70% ethanol and photographed.

For fluorometric GUS activity assays, 1-day-old imbibed rice seeds (imbibed for 2 h) were collected and homogenized in liquid nitrogen (Jefferson *et al*., 1987). The powder was resuspended in 500 μl GUS extraction buffer (50 mM sodium phosphate pH 7.0, 10 mM EDTA pH 8.0, 0.1% SDS, 0.1% Triton X-100). The supernatant after centrifugation was transferred to a new Eppendorf tube, and the concentration was determined by the Bradford assay. Fifty μl supernatant of rice seed extract were mixed with 250 μl reaction mix solution, containing 2 mM 4-MUG in GUS extraction buffer preheated to 37°C, in another Eppendorf tube. A 50-μl aliquot from the reaction tube was transferred to a new Eppendorf tube containing 950 μl stop reagent (1 M Na_2CO_3) at 10 min intervals (10, 20, and 30 min), respectively. Also, 100 nM, 250 nM, and 500 nM 4-MU was treated similar to construct a standard curve. GUS activity was examined using a spectrofluorometer (Bio-Tek FL600, Bio-Tek Instruments, Inc. USA) with excitation at 365 nm and emission at 455 nm. GUS activity was expressed in pmol 4-MU min^{-1} mg^{-1} protein.

Electrophoretic mobility shift assays (EMSAs)

Plant nuclear protein extraction was performed at 4°C using 5 g of 4-h imbibed 1-day-old rice seeds according to instructions from the Plant Nuclei Isolation/Extraction Kit (Sigma) with some modifications. biotin-labeled DNA probes were prepared as specified in the biotin 3′ End DNA Labeling Kit (Thermo Scientific). ML2564/ML2565 was used to generate probes containing Skn-l-like motif at −1486/−1482; ML2523/ML2524 for −956/−952 and −939/−935; ML2567/ML2568 for −826/−822; and ML2525/ML2526 for −766/−762 (Table S3). Mutagenized probes were designed by modifying 'GTCAT' to 'GGCCC' according to Washida *et al*. (1999). Mutagenized probes at the Skn-l-like motifs (Table S3) in which 'GTCAT' was replaced with 'GGCCC' were ML3188/ML3189 (−1486/−1482), ML3190/ML3191 (−956/−952 and −939/−935), ML3192/ML3193 (−826/−822), and ML3194/ML3195 (−766/−762).

EMSAs were carried out using the LightShift® Chemiluminescent EMSA Kit (ThermoFisher Scientific) following the manufacturer's instructions. Crude nuclear proteins (5 μg) from 1-day-old imbibed rice seeds were kept on ice in binding buffer containing 20 fM biotin-labeled DNA with or without 200-fold molar excess competitor oligonucleotide (non-labeled wild-type probes or biotin-labeled mutagenized probes) in a total volume of 20 μL. Poly [d(I-C)] (50 ng μL^{-1}) was added to reduce non-specific binding. A 6% native polyacrylamide gel was pre-run in 0.5 x Tris/Borate/EDTA (TBE) buffer at 100 V, 4°C for 1 h. Subsequently the binding mixtures were loaded and separated under the same voltage and temperature. The gel-run was terminated when the dye-front migrated to 3/4 down the length of the gel. The DNA and DNA–protein complex were blotted on a Hybond-N+ (GE Healthcare Life Sciences) nylon membrane. The membrane was washed and processed according to the manufacturer's instructions.

Generation of OsACBP2-overexpressing transgenic rice lines

To generate transgenic rice OsACBP2-OE plants, a 276-bp full-length *OsACBP2* cDNA from pOS499 (Meng *et al*., 2011) was cloned into the *Xcm*I sites of the binary vector pCXSN (Chen *et al*., 2009) to generate pOS691. The pOS691 (*35S:OsACBP2*) plant transformation vector was used for *Agrobacterium*-mediated rice transformation (Hiei *et al*., 1994). The transformed T_0 seeds were screened on MS medium containing hygromycin (50 μg ml^{-1}) and the resistant transformants were further confirmed by PCR using a *35S* promoter-specific forward primer 35SB and reverse *OsACBP2*-specific primer, ML1106 (Table S3). Out of a total 20 resultant transgenic lines analyzed by qRT-PCR and western blot analysis, four lines (OE-1, OE-3, OE-17, and OE-21) were identified to highly express OsACBP2. The T_3 homozygous lines from these four lines were used in phenotypic studies.

Germination tests

Germination tests were carried out in Petri dishes at 28°C. The seeds were incubated in darkness for the first 2 days. The cover was removed at 48 h after imbibition. Transgenic and wild-type rice seeds were then germinated in ½MS solid medium in a growth chamber in the dark at 28°C for a further 3 days, after which seedlings were soil-grown in a greenhouse (12-h light/12-h dark cycle) at 28 to 30°C. At maturity, the unfilled and filled grains were separately counted, measured and weighed.

Trait measurements

Grain length, width and weight were measured from completely mature plants. Grain length and width were determined using ImageJ software (https://imagej.nih.gov/ij/). After the seeds were dried at 37°C for 2 days, dry weight (DW) was measured. To determine fresh weight at different stages, 30 grains were weighed and measurements were repeated twice with another two sets of 30 grains. The *P*-values were computed using Student's *t*-test for traits of each rice line.

Arabidopsis seed size was measured according to Herridge *et al*. (2011). Briefly, 1000 seeds per genotype were scanned on a flatbed scanner (EPSON Perfection™ 1200 Photo) to capture the shadows cast by the seeds against a white background. The area of each shadow, representing seed size, was quantified using ImageJ (Schneider *et al*., 2012).

Transmission electron microscopy (TEM)

The ultrastructure of 1-day-old imbibed seeds from OsACBP2-OEs, *osacbp2* mutants, and WTs was examined by TEM following Sieber *et al*. (2000) with some modifications. Samples were fixed using 2.5% (v/v) glutaraldehyde and 1.6% (v/v) paraformaldehyde in 0.1 M sodium cacodylate-HCl buffer (pH7.4) overnight at 4°C, followed by post-fixation treatment with 1% (w/v) OsO_4 in cacodylate buffer for 2 h at room temperature. After gradient dehydration with ethanol, samples were infiltrated overnight with 1:1 (v/v) epoxy resin/propylene oxide mixture. Samples were subsequently embedded in epoxy resin and the resin polymerized overnight at 65°C. Ultrathin (60 nm) sections were prepared and stained with 2% (w/v) uranyl acetate and 2% (w/v) lead citrate, and subsequently examined using a Phillips CM100 transmission electron microscope.

Confocal microscopy

Confocal microscopy on rice aleurone cells was carried out as previously described (Hsiao *et al.*, 2014b) with modifications. Next 1-day-old imbibed rice seeds were infiltrated with an aqueous solution of Nile red (Sigma) to visualize lipid bodies in the rice aleurone. Images were obtained with a ×63 oil objective by confocal laser scanning microscopy using a Zeiss LSM 710 system equipped with argon and HeNe lasers as excitation sources. Fluorescence was excited at 514 nm and collected with a 539–653 nm filter. The resultant images were analyzed using ImageJ software (Schneider *et al.*, 2012).

Fatty acid analysis by gas chromatography–mass spectrometry (GC-MS)

FA analysis was conducted following Carvalho and Malcata (2005) with modifications. Here, 30 mg of lyophilized powder from rice dry seed was suspended, respectively, in a solution containing 1 ml of toluene, 2 ml of 1% (v/v) sulphuric acid in methanol together with 10 μl of internal standard [C19:0 (1 mg ml^{-1} in hexane)]. The mixtures were incubated for 12 h at 50°C for transmethylation of FAs. After several washes with 5% (w/v) NaCl and hexane, the hexane layer was washed with 4 ml of 2% (w/v) $NaHCO_3$ and then transferred into another test tube followed by vigorous vortexing. Nitrogen gas was blown into each tube to evaporate the hexane. Then 100 μl of hexane was re-added to the test tube to concentrate the FA residues. One μl of the hexane supernatant, containing the FAs, was analyzed by VT-WAXMS (Agilent Technologies) equipped with an HP-INNOWAX capillary column (HP19091N-133, 30 m x 0.25 nm × 0.25 μm). The samples were positioned and then automatically injected into the column. For sample detection, the oven temperature was increased from 100°C to 230°C with a rate of 4°C/min and post-run at 235°C for 4 min. The software GC/MSD On-line Data Analysis was used for data processing after data acquisition; the FAME library was used for compound identification. The limit of detection was determined to be 89.9 μg (~0.3% of average seed DW), calculated as 3σ for three blank samples (Guideline, 2005).

TAG analysis by electrospray ionization tandem triple-quadrupole mass spectrometry

Quantitative analyses of TAGs were carried out using electrospray ionization tandem triple-quadrupole mass spectrometry (4000 QTRAP; SCIX; ESI-MS/MS). For total lipid extraction, individual rice seeds (five replicates per line) were transferred to 1 ml of isopropanol, heated at 75°C and crushed with a glass rod. A further 1 ml each of chloroform, methanol and 0.8 ml of water was added, vortexed and centrifuged at 2000 rpm (3 min). The lower phase was removed to a fresh tube. The sample was re-extracted with 1 ml of chloroform and the lower phase combined with the first extraction. After drying with a stream of nitrogen the lipid extract was resuspended in 200 μl of chloroform in a glass vial and stored at −20°C for later analysis. The lipid extracts (10 μl of lipid extract combined with 990 μl of spray solvent) were infused at 15 μl min^{-1} with an auto-sampler (HTS-xt PAL, CTC-PAL Analytics AG, Switzerland). The ESI-MS/MS method described by Liang *et al.* (2014) was modified to quantify TAG contents. For quantifying TAG, 15 μl of lipid extract and 0.857 nmol of tri15:0-TAG (Nu-Chek Prep, Elysian, MN, USA) were combined with chloroform/methanol/300 mM ammonium acetate (24:24:1.75: v/v/v), to final volumes of 1 ml for direct infusion into the mass spectrometer. TAG molecular species were detected as $[M + NH_4]^+$ ions by a series of different neutral loss scans, targeting losses of FAs. The spectra were processed using the Lipid View Software (SCIEX, Framingham, MA, USA) in which isotope corrections were applied. The peak area of each lipid was normalized to the internal standard and further normalized to the weight of the initial sample. There was variation in ionization efficiency among the acyl glycerol species with different fatty acyl groups, and no response factors for individual species were determined in this study; therefore, the values are not directly proportional to the TAG contents of each species. However, the approach does allow a realistic comparison of TAG species across samples in this study.

ACKNOWLEDGEMENTS

We gratefully acknowledge the Rice Mutant Database (RMD; rmd.ncpgr.cn) and the Rice T-DNA Insertion Sequence Database (RISD DB; cbi.khu.ac.kr/RISD_DB.html) for provision of the *osacbp2* mutant rice seeds and Prof. Yongjun Lin (Huazhong Agricultural University) for binary vector DX2181. We thank Mr Rui Zhang for provision of the *OsACBP2*-overexpressing construct pOS691. This work was supported by the Wilson and Amelia Wong Endowment Fund (to M-LC), Research Grants Council of the Hong Kong Special Administrative Region, China (17105615M to M-LC), University of Hong Kong Postgraduate Studentship (to Z-HG), BBSRC (UK) Institute Strategic Programme Grants (BBS/E/C/000I0420 and BBS/E/C/00005207 to JAN, LVM, and RPH), Natural Sciences and Engineering Research Council of Canada (grant to ECY). Partial support from the Innovation Technology Fund of Innovation Technology Commission: Funding Support to State Key Laboratory of Agrobiotechnology (to M-LC) is also acknowledged.

AUTHOR CONTRIBUTIONS

ZHG performed most of the experiments. RPH and LVM performed TAG analysis. JAN supported lipid analyses. ZHG, RPH, ECY, SCL and MLC evaluated data. ZHG and MLC designed the research and wrote the manuscript with contribution from all authors.

CONFLICT OF INTEREST

The authors declare no conflict of interest.

DATA AVAILABILITY STATEMENT

All data generated and used in this study are available upon request or as Supporting Information in this article.

SUPPORTING INFORMATION

Additional Supporting Information may be found in the online version of this article.

Figure S1. Microarray analysis showing the relative expression levels of six *OsACBPs* in various organs.

Figure S2. *OsACBP2* is highly expressed in the embryos and endosperm of germinating wild-type rice seeds.

Figure S3. Electrophoretic mobility shift assays with non-biotin-labeled competitor showed no binding of nuclear extracts to the Skn-l-like motifs in the *OsACBP2* 5′-flanking region.

Figure S4. Characterization of four rice *osacbp2* mutants, RMD_03Z11AZ19, RMD_03Z11LE18, RMD_03Z11LG76, and PFG_1D-05815.

Figure S5. Germination tests on OsACBP2-OE and *osacbp2* lines.

Figure S6. Phenotypic analysis of OsACBP2-OE and *osacbp2* rice plants.

Figure S7. Confocal laser scanning microscopy of the aleurone cells from Nile red-stained imbibed rice seeds from *osacbp2*.

Figure S8. Transgenic Arabidopsis AtACBP6-OE lines and the *atacbp6* mutant do not differ in seed size from the Col-0 wild-type.

Table S1. Triacylglycerol (TAG) content (μmol mg^{-1}) of 1-day-old seeds from *osacbp2* mutants and OsACBP2-OEs by HPLC.

Table S2. Fatty acid content and composition of whole seeds from *osacbp2* mutants and OsACBP2-OEs.

Table S3. Sequence of oligonucleotide primers used in this study.

REFERENCES

Akihisa, T., Yasukawa, K., Yamaura, M., Ukiya, M., Kimura, Y., Shimizu, N. and Arai, K. (2000) Triterpene alcohol and sterol ferulates from rice bran and their anti-inflammatory effects. *J. Agric. Food Chem.* **48**, 2313–2319.

An, J.H. and Blackwell, T.K. (2003) SKN-1 links C-elegans mesendodermal specification to a conserved oxidative stress response. *Genes Dev.* **17**, 1882–1893.

Blackwell, T.K., Bowerman, B., Priess, J.R. and Weintraub, H. (1994) Formation of a monomeric DNA-binding domain by SKN-1 BZIP and homeodomain elements. *Science*, **266**, 621–628.

Bowerman, B., Eaton, B.A. and Priess, J.R. (1992) SKN-1, a maternally expressed gene required to specify the fate of ventral blastomeres in the early c-elegans embryo. *Cell*, **68**, 1061–1075.

Burton, M., Rose, T.M., Faergeman, N.J. and Knudsen, J. (2005) Evolution of the acyl-CoA binding protein (ACBP). *Biochem. J.* **392**, 299–307.

Carvalho, A.P. and Malcata, F.X. (2005) Preparation of fatty acid methyl esters for gas-chromatographic analysis of marine lipids: insight studies. *J. Agric. Food Chem.* **53**, 5049–5059.

Chapman, K.D., Dyer, J.M. and Mullen, R.T. (2012) Biogenesis and functions of lipid droplets in plants thematic review series: lipid droplet synthesis and metabolism: from yeast to man. *J. Lipid Res.* **53**, 215–226.

Chen, Q.-F., Xiao, S. and Chye, M.-L. (2008) Overexpression of the Arabidopsis 10-kilodalton acyl-coenzyme A-binding protein ACBP6 enhances freezing tolerance. *Plant Physiol.* **148**, 304–315.

Chen, S., Songkumarn, P., Liu, J. and Wang, G.-L. (2009) A versatile zero background T-vector system for gene cloning and functional genomics. *Plant Physiol.* **150**, 1111–1121.

Chen, Q.-F., Xiao, S., Qi, W.Q., Mishra, G., Ma, J.Y., Wang, M.F. and Chye, M.-L. (2010) The Arabidopsis *acbp1acbp2* double mutant lacking acyl-CoA-binding proteins ACBP1 and ACBP2 is embryo lethal. *New Phytol.* **186**, 843–855.

Chye, M.-L., Huang, B.-Q. and Zee, S.Y. (1999) Isolation of a gene encoding Arabidopsis membrane-associated acyl-CoA binding protein and immunolocalization of its gene product. *Plant J.* **18**, 205–214.

Clarke, N., Wilkinson, M. and Laidman, D. (1983) 4 lipid metabolism in germinating cereals. In *Lipids in Cereal Technology*. (Barnes, P.J., ed). New York: Academic Press, pp. 57–92.

Deng, Z.Y., Gong, C.Y. and Wang, T. (2013) Use of proteomics to understand seed development in rice. *Proteomics*, **13**, 1784–1800.

Du, Z.-Y. and Chye, M.-L. (2013) Interactions between Arabidopsis acyl-CoA-binding proteins and their protein partners. *Planta*, **238**, 239–245.

Du, H., Wang, N., Cui, F., Li, X., Xiao, J. and Xiong, L. (2010a) Characterization of the β-carotene hydroxylase gene *DSM2* conferring drought and oxidative stress resistance by increasing xanthophylls and abscisic acid synthesis in rice. *Plant Physiol.* **154**, 1304–1318.

Du, Z.-Y., Xiao, S., Chen, Q.-F. and Chye, M.-L. (2010b) Depletion of the membrane-associated acyl-coenzyme A-binding protein ACBP1 enhances the ability of cold acclimation in Arabidopsis. *Plant Physiol.* **152**, 1585–1597.

Du, Z.-Y., Chen, M.-X., Chen, Q.-F., Xiao, S. and Chye, M.-L. (2013a) Arabidopsis acyl-CoA-binding protein ACBP1 participates in the regulation of seed germination and seedling development. *Plant J.* **74**, 294–309.

Du, Z.-Y., Chen, M.-X., Chen, Q.-F., Xiao, S. and Chye, M.-L. (2013b) Overexpression of Arabidopsis acyl-CoA-binding protein ACBP2 enhances drought tolerance. *Plant, Cell Environ.* **36**, 300–314.

Du, Z.-Y., Arias, T., Meng, W. and Chye, M.-L. (2016) Plant acyl-CoA-binding proteins: an emerging family involved in plant development and stress responses. *Prog. Lipid Res.* **63**, 165–181.

Eastmond, P.J. (2006) SUGAR-DEPENDENT1 encodes a patatin domain triacylglycerol lipase that initiates storage oil breakdown in germinating Arabidopsis seeds. *Plant Cell*, **18**, 665–675.

Elert, E. (2014) Rice by the numbers: a good grain. *Nature*, **514**, S50–S51.

Elle, I.C., Simonsen, K.T., Olsen, L.C., Birck, P.K., Ehmsen, S., Tuck, S., Le, T.T. and Færgeman, N.J. (2011) Tissue-and paralogue-specific functions of acyl-CoA-binding proteins in lipid metabolism in *Caenorhabditis elegans*. *Biochem. J.* **437**, 231–241.

Fabian, C. and Ju, Y.-H. (2011) A review on rice bran protein: its properties and extraction methods. *Crit. Rev. Food Sci. Nutr.* **51**, 816–827.

Fang, N., Xu, R., Huang, L., Zhang, B., Duan, P., Li, N., Luo, Y. and Li, Y. (2016) SMALL GRAIN 11 controls grain size, grain number and grain yield in rice. *Rice*, **9**, 64.

FAO.ORG (2018a) *EST: Rice Market Monitor (RMM)*. Rome: Food and Agriculture Organization of the United Nations. http://www.fao.org/economic/est/publications/rice-publications/rice-market-monitor-rmm/en/

FAO.ORG (2018b) *FAO Cereal Supply and Demand Brief*. Rome: Food and Agriculture Organization of the United Nations. http://www.fao.org/worldfoodsituation/csdb/en/

Fauteux, F. and Stromvik, M.V. (2009) Seed storage protein gene promoters contain conserved DNA motifs in *Brassicaceae,* Fabaceae and Poaceae. *BMC Plant Biol.* **9**, 126.

Gao, W., Xiao, S., Li, H.-Y., Tsao, S.W. and Chye, M.-L. (2009) Arabidopsis thaliana acyl-CoA-binding protein ACBP2 interacts with heavy-metal-binding farnesylated protein AtFP6. *New Phytol.* **181**, 89–102.

Gao, W., Li, H.-Y., Xiao, S. and Chye, M.-L. (2010) Acyl-CoA-binding protein 2 binds lysophospholipase 2 and lysoPC to promote tolerance to cadmium-induced oxidative stress in transgenic Arabidopsis. *Plant J.* **62**, 989–1003.

Guideline, I.H.T. (2005) Validation of analytical procedures: text and methodology Q2 (R1). *International conference on harmonization*. Geneva: Switzerland, pp. 11–12.

Guo, Z.-H., Chan, W.H., Kong, G.K., Hao, Q. and Chye, M.-L. (2017) The first plant acyl-CoA-binding protein structures: the close homologues OsACBP1 and OsACBP2 from rice. *Acta Crystallogr. D* **73**, 438–448.

Halford, N.G. and Paul, M.J. (2003) Carbon metabolite sensing and signalling. *Plant Biotech. J.* **1**, 381–398.

Hernández, M.L., Whitehead, L., He, Z., Gazda, V., Gilday, A., Kozhevnikova, E., Vaistij, F.E., Larson, T.R. and Graham, I.A. (2012) A cytosolic acyltransferase contributes to triacylglycerol synthesis in sucrose-rescued Arabidopsis seed oil catabolism mutants. *Plant Physiol.* **160**, 215–225.

Herridge, R.P., Day, R.C., Baldwin, S. and Macknight, R.C. (2011) Rapid analysis of seed size in Arabidopsis for mutant and QTL discovery. *Plant Methods*, **7**, 3.

Hiei, Y., Ohta, S., Komari, T. and Kumashiro, T. (1994) Efficient transformation of rice (*Oryza sativa* L.) mediated by Agrobacterium and sequence analysis of the boundaries of the T-DNA. *Plant J.* **6**, 271–282.

Hong, Z., Ueguchi-Tanaka, M., Fujioka, S., Takatsuto, S., Yoshida, S., Hasegawa, Y., Ashikari, M., Kitano, H. and Matsuoka, M. (2005) The rice brassinosteroid-deficient dwarf2 mutant, defective in the rice homolog of Arabidopsis DIMINUTO/DWARF1, is rescued by the endogenously accumulated alternative bioactive brassinosteroid, dolichosterone. *Plant Cell*, **17**, 2243–2254.

Hsiao, A.-S., Haslam, R.P., Michaelson, L.V., Liao, P., Chen, Q.-F., Sooriyaarachchi, S., Mowbray, S.L., Napier, J.A., Tanner, J.A. and Chye, M.-L. (2014a) Arabidopsis cytosolic acyl-CoA-binding proteins ACBP4, ACBP5 and ACBP6 have overlapping but distinct roles in seed development. *Biosci. Rep.* **34**, 865–877.

Hsiao, A.-S., Haslam, R.P., Michaelson, L.V., Liao, P., Napier, J.A. and Chye, M.-L. (2014b) Gene expression in plant lipid metabolism in Arabidopsis seedlings. *PLoS ONE*, **9**, e107372.

Hsiao, A.-S., Yeung, E.C., Ye, Z.-W. and Chye, M.-L. (2015) The Arabidopsis cytosolic acyl-CoA-binding proteins play combinatory roles in pollen development. *Plant Cell Physiol.* **56**, 322–333.

Hu, T.-H., Lung, S.-C., Ye, Z.-W. and Chye, M.-L. (2018) Depletion of Arabidopsis ACYL-CoA-BINDING PROTEIN3 affects fatty acid composition in the phloem. *Front. Plant Sci.* **9**, 2.

Jako, C., Kumar, A., Wei, Y., Zou, J., Barton, D.L., Giblin, E.M., Covello, P.S. and Taylor, D.C. (2001) Seed-specific over-expression of an Arabidopsis cDNA encoding a diacylglycerol acyltransferase enhances seed oil content and seed weight. *Plant Physiol.* **126**, 861–874.

Jefferson, R.A., Kavanagh, T.A. and Bevan, M.W. (1987) GUS fusions - beta-glucuronidase as a sensitive and versatile gene fusion marker in higher-plants. *EMBO J.* **6**, 3901–3907.

Khush, G.S. (2005) What it will take to feed 5.0 billion rice consumers in 2030. *Plant Mol. Biol.* **59**, 1–6.

Khush, G.S. (2013) Strategies for increasing the yield potential of cereals: case of rice as an example. *Plant Breed.* **132**, 433–436.

Kragelund, B.B., Andersen, K.V., Madsen, J.C., Knudsen, J. and Poulsen, F.M. (1993) 3-dimensional structure of the complex between acyl-coenzyme-A binding-protein and palmitoyl-coenzyme-a. *J. Mol. Biol.* **230**, 1260–1277.

Landrock, D., Atshaves, B.P., McIntosh, A.L., Landrock, K.K., Schroeder, F. and Kier, A.B. (2010) Acyl-CoA binding protein gene ablation induces pre-implantation embryonic lethality in mice. *Lipids*, **45**, 567–580.

Lescot, M., Déhais, P., Thijs, G., Marchal, K., Moreau, Y., Van de Peer, Y., Rouzé, P. and Rombauts, S. (2002) PlantCARE, a database of plant *cis*-acting regulatory elements and a portal to tools for *in silico* analysis of promoter sequences. *Nucleic Acids Res.* **30**, 325–327.

Leung, K.C., Li, H.-Y., Xiao, S., Tse, M.H. and Chye, M.-L. (2006) Arabidopsis ACBP3 is an extracellularly targeted acyl-CoA-binding protein. *Planta*, **223**, 871–881.

Li, H.-Y. and Chye, M.-L. (2003) Membrane localization of Arabidopsis acyl-CoA binding protein ACBP2. *Plant Mol. Biol.* **51**, 483–492.

Li, Y.B., Fan, C.C., Xing, Y.Z. *et al.* (2011) Natural variation in *GS5* plays an important role in regulating grain size and yield in rice. *Nature Genet.* **43**, 1266–1269.

Liang, C., Wang, Y., Zhu, Y. *et al.* (2014) OsNAP connects abscisic acid and leaf senescence by fine-tuning abscisic acid biosynthesis and directly targeting senescence-associated genes in rice. *Proc. Natl Acad. Sci. USA* **111**, 10013–10018.

Liao, P., Chen, Q.-F. and Chye, M.-L. (2014) Transgenic Arabidopsis flowers overexpressing acyl-CoA-binding protein ACBP6 are freezing tolerant. *Plant Cell Physiol.* **55**, 1055–1071.

Liao, P.-F., Ouyang, J.-X., Zhang, J.-J., Yang, L., Wang, X., Peng, X.-J., Wang, D., Zhu, Y.-L. and Li, S.-B. (2019) OsDCL3b affects grain yield and quality in rice. *Plant Mol. Biol.* **99**, 193–204.

Liu, J., Chen, J., Zheng, X., Wu, F., Lin, Q., Heng, Y., Tian, P., Cheng, Z., Yu, X. and Zhou, K. (2017) *GW5* acts in the brassinosteroid signalling pathway to regulate grain width and weight in rice. *Nat. Plants*, **3**, 17043.

Lu, C.A., Lin, C.C., Lee, K.W., Chen, J.L., Huang, L.F., Ho, S.L., Liu, H.J., Hsing, Y.I. and Yu, S.M. (2007) The SnRK1A protein kinase plays a key role in sugar signaling during germination and seedling growth of rice. *Plant Cell*, **19**, 2484–2499.

Lung, S.-C. and Chye, M.-L. (2016a) Acyl-CoA-binding proteins (ACBPs) in plant development. In *Lipids in Plant and Algae Development*. (Nakamura, Y. and Li-Beisson, Y., eds). Cham: Springer, pp. 363–404.

Lung, S.-C. and Chye, M.-L. (2016b) The binding versatility of plant acyl-CoA-binding proteins and their significance in lipid metabolism. *Biochim. Biophys. Acta Mol. Cell. Biol. Lipids* **1861**, 1409–1421.

Lung, S.-C. and Chye, M.-L. (2016c) Deciphering the roles of acyl-CoA-binding proteins in plant cells. *Protoplasma*, **253**, 1177–1195.

Lung, S.-C., Liao, P., Yeung, E.C.-T., Hsiao, A.-S., Xue, Y. and Chye, M.-L. (2017) Acyl-CoA-binding protein ACBP1 modulates sterol synthesis during embryogenesis. *Plant Physiol.* **174**, 1420–1435.

Lung, S.C., Liao, P., Yeung, E.C., Hsiao, A.S., Xue, Y. and Chye, M.L. (2018) Arabidopsis ACYL-COA-BINDING PROTEIN1 interacts with STEROL C4-METHYL OXIDASE1-2 to modulate gene expression of homeodomain-leucine zipper IV transcription factors. *New Phytol.* **218**, 183–200.

Majerowicz, D., Hannibal-Bach, H.K., Castro, R.S., Bozaquel-Morais, B.L., Alves-Bezerra, M., Grillo, L.A., Masuda, C.A., Færgeman, N.J., Knudsen, J. and Gondim, K.C. (2016) The ACBP gene family in *Rhodnius prolixus*: expression, characterization and function of RpACBP-1. *Insect Biochem. Mol. Biol.* **72**, 41–52.

Mansfield, S.G. and Briarty, L.G. (1992) Cotyledon cell development in *Arabidopsis thaliana* during reserve deposition. *Can. J. Bot.* **70**, 151–164.

Mao, H.L., Sun, S.Y., Yao, J.L., Wang, C.R., Yu, S.B., Xu, C.G., Li, X.H. and Zhang, Q.F. (2010) Linking differential domain functions of the GS3 protein to natural variation of grain size in rice. *Proc. Natl Acad. Sci. USA* **107**, 19579–19584.

Meng, W., Su, Y.C.F., Saunders, R.M.K. and Chye, M.-L. (2011) The rice acyl-CoA-binding protein gene family: phylogeny, expression and functional analysis. *New Phytol.* **189**, 1170–1184.

Montesinos, L., Bundó, M., Izquierdo, E., Campo, S., Badosa, E., Rossignol, M., Montesinos, E., San Segundo, B. and Coca, M. (2016) Production of biologically active Cecropin A peptide in rice seed Oil bodies. *PLoS ONE*, **11**, e0146919.

Morinaka, Y., Sakamoto, T., Inukai, Y., Agetsuma, M., Kitano, H., Ashikari, M. and Matsuoka, M. (2006) Morphological alteration caused by brassinosteroid insensitivity increases the biomass and grain production of rice. *Plant Physiol.* **141**, 924–931.

Murphy, D.J. (1994) Biogenesis, function and biotechnology of plant storage lipids. *Prog. Lipid Res.* **33**, 71–85.

Nagasaka, R., Yamsaki, T., Uchida, A., Ohara, K. and Ushio, H. (2011) γ-Oryzanol recovers mouse hypoadiponectinemia induced by animal fat ingestion. *Phytomedicine*, **18**, 669–671.

Napier, J.A. and Haslam, R.P. (2010) As simple as ACB–new insights into the role of acyl-CoA-binding proteins in Arabidopsis. *New Phytol.* **186**, 781–783.

Ohlrogge, J. and Browse, J. (1995) Lipid biosynthesis. *Plant Cell*, **7**, 957–970.

Pyc, M., Cai, Y., Greer, M.S., Yurchenko, O., Chapman, K.D., Dyer, J.M. and Mullen, R.T. (2017) Turning over a new leaf in lipid droplet biology. *Trends Plant Sci.* **22**, 596–609.

Ray, D.K., Mueller, N.D., West, P.C. and Foley, J.A. (2013) Yield trends are insufficient to double global crop production by 2050. *PLoS ONE*, **8**, e66428.

Rong, N., Ausman, L.M. and Nicolosi, R.J. (1997) Oryzanol decreases cholesterol absorption and aortic fatty streaks in hamsters. *Lipids*, **32**, 303–309.

Sambrook, J., Fritsch, E.F. and Maniatis, T. (1989) *Molecular Cloning: A Laboratory Manual*. New York: Cold Spring Harbor.

Sato, Y., Antonio, B.A., Namiki, N., Takehisa, H., Minami, H., Kamatsuki, K., Sugimoto, K., Shimizu, Y., Hirochika, H. and Nagamura, Y. (2010) RiceX-Pro: a platform for monitoring gene expression in *japonica* rice grown under natural field conditions. *Nucleic Acids Res.* **39**, D1141–D1148.

Schneider, C.A., Rasband, W.S. and Eliceiri, K.W. (2012) NIH Image to ImageJ: 25 years of image analysis. *Nat. Methods*, **9**, 671.

Segami, S., Kono, I., Ando, T., Yano, M., Kitano, H., Miura, K. and Iwasaki, Y. (2012) *Small and round seed 5* gene encodes alpha-tubulin regulating seed cell elongation in rice. *Rice*, **5**, 4.

Shomura, A., Izawa, T., Ebana, K., Ebitani, T., Kanegae, H., Konishi, S. and Yano, M. (2008) Deletion in a gene associated with grain size increased yields during rice domestication. *Nat. Genet.* **40**, 1023–1028.

Si, L., Chen, J., Huang, X., Gong, H., Luo, J., Hou, Q., Zhou, T., Lu, T., Zhu, J. and Shangguan, Y. (2016) *OsSPL13* controls grain size in cultivated rice. *Nat. Genet.* **48**, 447–456.

Sieber, P., Schorderet, M., Ryser, U., Buchala, A., Kolattukudy, P., Métraux, J.P. and Nawrath, C. (2000) Transgenic Arabidopsis plants expressing a fungal cutinase show alterations in the structure and properties of the cuticle and postgenital organ fusions. *Plant Cell*, **12**, 721–737.

Siloto, R.M.P., Findlay, K., Lopez-Villalobos, A., Yeung, E.C., Nykiforuk, C.L. and Moloney, M.M. (2006) The accumulation of oleosins determines the size of seed oilbodies in Arabidopsis. *Plant Cell*, **18**, 1961–1974.

Song, X.J., Huang, W., Shi, M., Zhu, M.Z. and Lin, H.X. (2007) A QTL for rice grain width and weight encodes a previously unknown RING-type E3 ubiquitin ligase. *Nat. Genet.* **39**, 623–630.

Spoel, S.H., Koornneef, A., Claessens, S.M., Korzelius, J.P., Van Pelt, J.A., Mueller, M.J., Buchala, A.J., Métraux, J.-P., Brown, R. and Kazan, K. (2003) NPR1 modulates cross-talk between salicylate-and jasmonate-dependent defense pathways through a novel function in the cytosol. *Plant Cell*, **15**, 760–770.

Tanabe, S., Ashikari, M., Fujioka, S., Takatsuto, S., Yoshida, S., Yano, M., Yoshimura, A., Kitano, H., Matsuoka, M. and Fujisawa, Y. (2005) A novel cytochrome P450 is implicated in brassinosteroid biosynthesis via the characterization of a rice dwarf mutant, dwarf11, with reduced seed length. *Plant Cell*, **17**, 776–790.

Taskinen, J.P., van Aalten, D.M., Knudsen, J. and Wierenga, R.K. (2007) High resolution crystal structures of unliganded and liganded human liver ACBP reveal a new mode of binding for the acyl-CoA ligand. *Proteins: Struct., Funct., Bioinf.* **66**, 229–238.

Wang, S.K., Li, S., Liu, Q. *et al.* (2015a) The *OsSPL16-GW7* regulatory module determines grain shape and simultaneously improves rice yield and grain quality. *Nat. Genet.* **47**, 949–954.

Wang, Y.X., Xiong, G.S., Hu, J. *et al.* (2015b) Copy number variation at the *GL7* locus contributes to grain size diversity in rice. *Nat. Genet.* **47**, 944–948.

Washida, H., Wu, C.-Y., Suzuki, A., Yamanouchi, U., Akihama, T., Harada, K. and Takaiwa, F. (1999) Identification of *cis*-regulatory elements required for endosperm expression of the rice storage protein glutelin gene *GluB-1*. *Plant Mol. Biol.* **40**, 1–12.

Weselake, R.J., Taylor, D.C., Rahman, M.H., Shah, S., Laroche, A., McVetty, P.B. and Harwood, J.L. (2009) Increasing the flow of carbon into seed oil. *Biotechnol. Adv.* **27**, 866–878.

Wilson, T.A., Nicolosi, R.J., Woolfrey, B. and Kritchevsky, D. (2007) Rice bran oil and oryzanol reduce plasma lipid and lipoprotein cholesterol concentrations and aortic cholesterol ester accumulation to a greater extent than ferulic acid in hypercholesterolemic hamsters. *J. Nutr. Biochem.* **18**, 105–112.

Woolston, C. (2014) Rice. *Nature*, **514**, S49.

Xiao, S. and Chye, M.L. (2009) An Arabidopsis family of six acyl-CoA-binding proteins has three cytosolic members. *Plant Physiol. Biochem.* **47**, 479–484.

Xiao, S. and Chye, M.-L. (2011) New roles for acyl-CoA-binding proteins (ACBPs) in plant development, stress responses and lipid metabolism. *Prog. Lipid Res.* **50**, 141–151.

Xiao, S., Gao, W., Chen, Q.F., Chan, S.W., Zheng, S.X., Ma, J.Y., Wang, M.F., Welti, R. and Chye, M.L. (2010) Overexpression of Arabidopsis Acyl-CoA binding protein ACBP3 promotes starvation-induced and age-dependent leaf senescence. *Plant Cell*, **22**, 1463–1482.

Xu, Z., Hua, N. and Godber, J.S. (2001) Antioxidant activity of tocopherols, tocotrienols, and γ-Oryzanol components from rice bran against cholesterol oxidation accelerated by 2, 2′-Azobis (2-methylpropionamidine) dihydrochloride. *J. Agric. Food Chem.* **49**, 2077–2081.

Xue, Y., Xiao, S., Kim, J., Lung, S.-C., Chen, L., Tanner, J.A., Suh, M.C. and Chye, M.-L. (2014) Arabidopsis membrane-associated acyl-CoA-binding protein ACBP1 is involved in stem cuticle formation. *J. Exp. Bot.* **65**, 5473–5483.

Yang, J., Cho, L.-H., Yoon, J. *et al.* (2019) Chromatin interacting factor OsVIL2 increases biomass and rice grain yield. *Plant Biotech. J.* **17**, 178–187.

Yasukawa, K., Akihisa, T., Kimura, Y., Tamura, T. and Takido, M. (1998) Inhibitory effect of cycloartenol ferulate, a component of rice bran, on tumor promotion in two-stage carcinogenesis in mouse skin. *Biol. Pham. Bull.* **21**, 1072–1076.

Ye, Z.-W. and Chye, M.-L. (2016) Plant cytosolic acyl-CoA-binding proteins. *Lipids*, **51**, 1–13.

Yuan, H., Fan, S., Huang, J., Zhan, S., Wang, S., Gao, P., Chen, W., Tu, B., Ma, B. and Wang, Y. (2017) 08SG2/OsBAK1 regulates grain size and number, and functions differently in Indica and Japonica backgrounds in rice. *Rice*, **10**, 25.

Zhou, Y., Atkins, J.B., Rompani, S.B., Bancescu, D.L., Petersen, P.H., Tang, H., Zou, K., Stewart, S.B. and Zhong, W. (2007) The mammalian Golgi regulates numb signaling in asymmetric cell division by releasing ACBD3 during mitosis. *Cell*, **129**, 163–178.

Zhou, Y., Tao, Y., Zhu, J., Miao, J., Liu, J., Liu, Y., Yi, C., Yang, Z., Gong, Z. and Liang, G. (2017) GNS4, a novel allele of DWARF11, regulates grain number and grain size in a high-yield rice variety. *Rice*, **10**, 34.

Zhu, X.L., Liang, W.Q., Cui, X., Chen, M.J., Yin, C.S., Luo, Z.J., Zhu, J.Y., Lucas, W.J., Wang, Z.Y. and Zhang, D.B. (2015) Brassinosteroids promote development of rice pollen grains and seeds by triggering expression of Carbon Starved Anther, a MYB domain protein. *Plant J.* **82**, 570–581.